The Canadian Mineralogist
Vol. 50, pp. 593-609 (2012)
DOI: 10.3749/canmin.50.3.593

CRYSTAL CHEMISTRY OF MINERALS OF THE WÖHLERITE GROUP FROM THE LOS ARCHIPELAGO, GUINEA

CRISTIAN BIAGIONI§ AND STEFANO MERLINO

Dipartimento di Scienze della Terra – Università di Pisa, Via Santa Maria 53, I-56126 Pisa, Italy

GIAN CARLO PARODI

Laboratoire de Minéralogie et Cosmochimie du Muséum UMR 7160, Muséum National d'Histoire Naturelle, 61 rue Buffon, F-75005 Paris, France

NATALE PERCHIAZZI[1]

Dipartimento di Scienze della Terra – Università di Pisa, Via Santa Maria 53, I-56126 Pisa, Italy

ABSTRACT

As part of the SYNTHESYS European project, a suite of samples from the nepheline syenites of the Los Archipelago, Guinea, was studied in order to characterize the crystal chemistry of the minerals belonging to the wöhlerite group. Chemical and X-ray studies permitted the identification of four different mineral species: låvenite, normandite, wöhlerite, and hiortdahlite I. The identification of hiortdahlite II reported by Robles *et al*. (2001) seems to be questionable.

Låvenite and normandite occur in the agpaitic suite, in association with analcime, catapleiite, fluorite, mosandrite, sérandite, sphalerite, and villiaumite; wöhlerite and hiortdahlite I are associated with britholite-(Ce), magnetite, titanite, and zircon.

All the studied låvenite and normandite crystals are intermediate terms in the låvenite-normandite series. Wöhlerite shows the highest Mn content ever recorded for this species. Hiortdahlite I is the poorest in terms of both Zr and Na content and the richest in Ca and F among the known occurrences of "hiortdahlite".

The crystal structures of these four phases were refined, with *R* factors ranging from 1.9% (for Mn-rich wöhlerite) to 7.3% (for hiortdahlite I).

The wide range in Zr-Ti ratios observed in the låvenite-normandite series using new data and all available chemical data, not reported in other Zr-Ti minerals, seems to be related to the contemporaneous substitution of Mn by Ca.

The comparison of the geometry of (Nb,Ti)- and Zr-centered polyhedra, including all the available structural studies of the wöhlerite group, indicates it is possible to make a distinction between (Nb,Ti)-dominant and Zr-dominant sites in this mineral family.

Keywords: låvenite, normandite, wöhlerite, hiortdahlite I, agpaitic syenite, Los Archipelago, Guinea

INTRODUCTION

The Los Archipelago, located 5 km offshore of Conakry, capital of Guinea, is mainly formed by nepheline syenites emplaced in the West African continental margin during Albian time (Moreau *et al*. 1996). This magmatic complex is similar to other alkaline massifs, such as Ilímaussaq in south Greenland; Mont Saint-Hilaire, Québec, Canada; and the Khibiny and Lovozero massifs in Kola Peninsula, Russia.

The mineralogy of the Los Archipelago was studied by Lacroix (Lacroix 1911), who first described villiaumite (Lacroix 1908) and sérandite (Lacroix 1931). Parodi & Chevrier (2004) reported the occurrence of some unknown Zr-Ti silicates; one of them was subsequently described as the new mineral roumaite by Biagioni *et al*. (2010a). The Zr-Ti-Nb-REE disilicates from the Los Archipelago belong to two distinct groups of minerals, *i.e*., the wöhlerite group and the mosandrite group. As shown in Table 1, both groups are characterized by the general formula $M_8(Si_2O_7)_2(O,OH,F)_4$, where *M* represents a wide range of cations with variable charges and ionic radii, typically six- to eight-fold coordinated. As pointed out by Bellezza *et al*.

§ E-mail address: biagioni@dst.unipi.it

(2004b), the above general formula can also describe the chemistry of another group of disilicates, *i.e.*, the rosenbuschite group.

These three groups of minerals differ for their structural arrangements (Fig. 1), that can be described in modular terms. The crystal structure of the members of the wöhlerite group (Fig. 1a) is formed by two kinds of modules, *i.e.*, walls of "octahedra", four columns large and extending along [001], and disilicate groups (Merlino & Perchiazzi 1988). In the rosenbuschite group (Fig. 1b), besides disilicate groups, "octahedral" cations are arranged by edge sharing into layers (*O* layers) and ribbons. Heterogeneous layers (*H* layers) formed by octahedral ribbons and disilicate groups alternate with the *O* layers, into a layered *HOH* structure (Christiansen *et al.* 2003b). Lastly, minerals belonging to the mosandrite group (Fig. 1c) are characterized by three kinds of modules: (1) layers of seven-fold coordinated polyhedra, analogous to those occurring in the minerals of the tobermorite group (Merlino *et al.* 1999); (2) "octahedral" layers, resembling the *O* layers of rosenbuschite group; and (3) disilicate groups.

The minerals of the three above mentioned groups are typically found as rare accessories in agpaitic syenites and carbonatites. They are usually identified only on the basis of EDS and WDS chemical analyses; as an example, see the studies by Ferguson (1978), Woolley & Platt (1986), Mariano & Roeder (1989), Keller *et al.* (1995), and Coulson (1997). In view of the wide chemical variability inside each of these mineral groups, an unambiguous identification is instead possible only by coupling chemical data with X-ray diffraction studies. X-ray powder diffraction data can readily indicate the mineral group to which a given phase belongs, whereas, owing to the modular character of these phases, a full identification of the mineral species is possible only through single-crystal X-ray diffraction studies coupled with chemical analyses.

As part of the SYNTHESYS European project (FR-TAF-2137: "Crystallography and crystal chemistry of rare Zr-Ti-Nb phases from the Iles de Los, Guinea"), we investigated a suite of samples kept in the Muséum National d'Histoire Naturelle of Paris and labeled as members of the wöhlerite group from the Los Archi-

TABLE 1. MINERAL SPECIES BELONGING TO THE MOSANDRITE, ROSENBUSCHITE, AND WÖHLERITE GROUPS

Name	Formula	*a* (Å)	*b* (Å)	*c* (Å)	α (°)	β (°)	γ (°)	s.g.	*Z*	Ref.
mosandrite group										
dovyrenite	$Ca_6Zr[Si_2O_7]_2(OH)_4$	5.666	18.844	3.728				*Pnnm*	1	[1]
mosandrite	$Ti(\square,Ca,Na)_3(Ca,REE)_4(Si_2O_7)_2[H_2O,OH,F]_4 \cdot \sim 1H_2O$	7.398	5.595	18.662	90	101.37	90	$P2_1/c$	2	[2]
nacareniobsite-(Ce)	$NbNa_3Ca_3REE(Si_2O_7)_2OF_3$	7.468	5.689	18.891	90	101.37	90	$P2_1/c$	2	[3]
rinkite	$TiNa_2Ca_4REE(Si_2O_7)_2OF_3$	7.433	5.660	18.818	90	101.35	90	$P2_1/c$	2	[4]
roumaite	$(Nb,Ti)(Ca,Na,\square)_3(Ca,REE)_4(Si_2O_7)_2(OH)F_3$	7.473	11.294	18.778	90	101.60	90	*Cc*	4	[5]
rosenbuschite group										
götzenite	$NaCa_6Ti(Si_2O_7)_2OF_3$	9.619	5.725	7.331	89.92	101.13	100.64	*P*-1	1	[6, 7]
grenmarite	$Na_4MnZr_3(Si_2O_7)_2O_2F_2$	5.608	7.139	18.575	90	102.60	90	*P*2/*c*	2	[7, 8]
hainite	$Na_2Ca_4(Y,REE)Ti(Si_2O_7)_2OF_3$	9.584	7.267	5.708	89.85	101.22	101.03	*P*-1	1	[6, 7]
kochite	$Na_3Ca_2MnZrTi(Si_2O_7)_2OF_3$	10.032	11.333	7.202	90.19	100.33	111.55	*P*-1	2	[7, 9]
rosenbuschite	$Na_6Ca_6Zr_3Ti(Si_2O_7)_4O_2F_6$	10.137	11.398	7.271	90.22	100.31	111.87	*P*-1	1	[6, 7]
seidozerite	$Na_4MnZr_2Ti(Si_2O_7)_2O_2F_2$	5.556	7.075	18.406	90	102.71	90	*P*2/*c*	2	[6, 7]
wöhlerite group										
baghdadite	$Ca_6Zr_2(Si_2O_7)_2O_4$	10.432	10.163	7.356	90	90.96	90	$P2_1/a$	2	[10]
burpalite	$Na_4Ca_2Zr_2(Si_2O_7)_2F_4$	10.117	10.445	7.256	90	90.04	90	$P2_1/a$	2	[11]
cuspidine	$Ca_8(Si_2O_7)_2F_4$	10.906	10.521	7.518	90	109.30	90	$P2_1/a$	2	[12]
hiortdahlite I	$(Na,Ca)_2Ca_4Zr(Mn,Ti,Fe)(Si_2O_7)_2(F,O)_4$	11.015	10.941	7.353	109.35	109.88	83.43	*P*-1	2	[13]
hiortdahlite II	$Na_2Ca_4Zr(Y,Zr,Mn,Fe)(Si_2O_7)_2(F,O)_4$	11.012	10.342	7.359	89.92	109.21	90.06	*P*-1	2	[14]
janhaugite	$Na_3Mn_3Ti_2(Si_2O_7)_2(O,OH,F)_4$	10.668	9.787	13.931	90	107.82	90	$P2_1/n$	4	[15]
låvenite	$(Na,Ca)_4(Mn,Fe)_2(Zr,Ti,Nb)_2(Si_2O_7)_2(O,F)_4$	10.83	9.98	7.174	90	108.1	90	$P2_1/a$	2	[16]
marianoite	$Na_2Ca_4(Nb,Zr)_2(Si_2O_7)_2(O,F)_4$	10.846	10.226	7.273	90	109.33	90	$P2_1$	2	[17]
niocalite	$Ca_7Nb(Si_2O_7)_2O_3F$	10.863	10.431	7.370	90	110.1	90	*Pa*	2	[18]
normandite	$Na_2Ca_2(Mn,Fe)_2(Ti,Nb,Zr)_2(Si_2O_7)_2O_2F_2$	10.799	9.801	7.054	90	108.08	90	$P2_1/a$	2	[19]
wöhlerite	$Na_2Ca_4Zr(Nb,Ti)(Si_2O_7)_2(O,F)_4$	10.823	10.244	7.290	90	109.00	90	$P2_1$	2	[20]

[1] Kadiyski *et al.* 2008; [2] Bellezza *et al.* 2009; [3] Sokolova & Hawthorne 2008; [4] Cámara *et al.* 2011; [5] Biagioni *et al.* 2010a; [6] Christiansen *et al.* 2003b; [7] Sokolova 2006; [8] Bellezza *et al.* 2004a; [9] Christiansen *et al.* 2003a; [10] Biagioni *et al.* 2010b; [11] Merlino *et al.* 1990; [12] Saburi *et al.* 1977; [13] Merlino & Perchiazzi 1985; [14] Merlino & Perchiazzi 1987; [15] Annehed *et al.* 1985; [16] Mellini 1981; [17] Chakhmouradian *et al.* 2008; [18] Mellini 1982; [19] Perchiazzi *et al.* 2000; [20] Mellini & Merlino 1979.

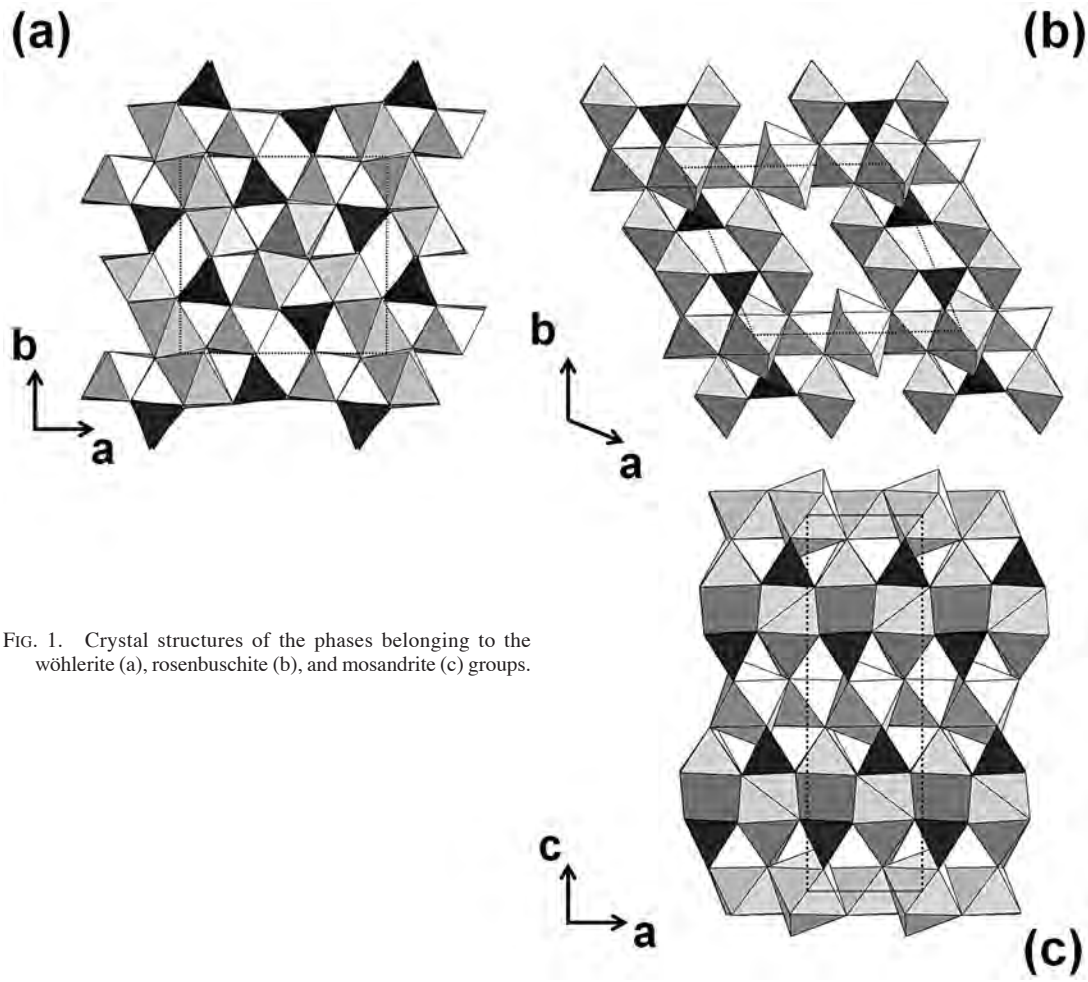

FIG. 1. Crystal structures of the phases belonging to the wöhlerite (a), rosenbuschite (b), and mosandrite (c) groups.

pelago, characterizing them both through chemical and X-ray diffraction studies, so to ascertain the true nature of these minerals.

MINERALS OF THE WÖHLERITE GROUP: AN OVERVIEW

The wöhlerite group (so-called from the first described mineral species, wöhlerite; Scheerer 1843) includes eleven minerals (Table 1) with monoclinic or triclinic symmetry. As stated above, the crystal structure of these phases can be described as the assemblage of two distinct modules.

The walls of "octahedra" are interconnected both directly by corner-sharing and through Si_2O_7 groups, each group being linked to three walls. The various minerals differ according to two basic features: (1) the different way of connecting the disilicate groups to the walls of "octahedra" and (2) the cation distributions within the walls (Merlino & Perchiazzi 1988).

Merlino & Perchiazzi (1988) showed that within unit-cell dimensions of ~10 × ~10 × ~7.3 Å^3, ten different topological structure types exist, corresponding to the ten distinct ways in which the disilicate groups can be connected to the framework of octahedra; these ten structure types can be distributed among four distinct types of unit-cell. The actual space group symmetry depends on the topological symmetry and the cation distribution within the walls of "octahedra" (Merlino & Perchiazzi 1988).

Minerals belonging to the wöhlerite group are common accessory phases in nepheline syenites from localities worldwide, *i.e.*, Poços de Caldas, Brazil (Atencio *et al.* 1999); Mont Saint-Hilaire (Horváth & Gault 1990) and Varennes (Horváth *et al.* 1998), both in Québec, Canada; the Eifel volcanic region, Germany (Hentschel 1986); Langesundsfjord, Norway (Brögger 1890); the Agua de Pau volcano, Azore Islands (Ridolfi *et al.* 2003); and the Khibiny and Lovozero massifs,

Russia (Vlasov *et al.* 1966). Regarding the occurrence of minerals of the wöhlerite group in the Los Archipelago, several investigators (Lacroix 1924, Lazarenkov 1975, Moreau *et al.* 1996, Robles *et al.* 2001) described their occurrence in the agpaitic *facies* of the syenites.

Identification of the Specimens from Los Archipelago

Description of samples

The crystal morphology of the minerals belonging to the wöhlerite group from the Los Archipelago ranges from prismatic to acicular, always with a good prismatic cleavage. According to differences in their colors, three types of phases have been distinguished: (1) Type A: prismatic to acicular crystals, up to 1 cm in length, with color ranging from honey-yellow to orange. In some cases, crystals form radial aggregates. This type corresponds to specimens labeled as låvenite (specimens 106.211 and 131.80) and LOS 180; (2) Type B: yellow prismatic crystals, up to 0.8 mm long, labeled as wöhlerite (specimens 111.6 and 113.119); (3) Type C: whitish prismatic crystals, labeled as "hiortdahlite" (specimen 119.115). This specimen is the same as that studied by Robles *et al.* (2001) and identified as hiortdahlite II on the basis of X-ray powder diffraction data alone.

The crystals of type A are associated with analcime, catapleiite, fluorite, mosandrite, sérandite, sphalerite, and villiaumite, a typical mineral assemblage for the agpaitic suite (Moreau *et al.* 1996). On the contrary, grains of type B and C are associated with britholite-(Ce), magnetite, titanite, and zircon.

Preliminary X-ray diffraction studies and qualitative chemical analyses

The crystals were preliminarily tested by X-ray powder diffraction using a 114.6 mm Gandolfi camera and Ni-filtered Cu$K\alpha$ radiation. Powder patterns clearly indicated that the investigated crystals belong to the wöhlerite group. Subsequent X-ray single-crystal studies were performed using the Weissenberg technique, collecting, as suggested by Merlino & Perchiazzi (1988), photographs of the reciprocal layers *hk*0 and *hk*1, so as to verify which of the four possible cell types was realized.

Crystals of type A show a type-I cell and systematic absences indicate space group $P12_1/a1$. Crystals of type B have a type-II cell; in this case, the systematic absences suggest space group $P2_111$ ($P2_1/m11$ may be ruled out, following Merlino & Perchiazzi 1988). Finally, crystals of type C display a type-IV cell. No systematic absences were observed, in agreement with a possible *P*-1 space group. Therefore, the identification of hiortdahlite II given by Robles *et al.* (2001) is incorrect, as hiortdahlite II has a type-I cell, whereas crystals from specimen 119.115 display a type-IV cell.

Qualitative EDS chemical analyses, collected using a Philips XL30 SEM, equipped with an EDAX DX4 system, show the following chemical features: (1) the A type shows Na ≈ Ca, Zr >> Nb; Mn > Ti ≈ Fe; the analysis of a crystal of specimen LOS 180 showed a remarkably greater Ti content than those shown by the other two specimens (106.211 and 131.80); (2) the B type shows Ca > Na; Zr ≈ Nb; minor amounts of Mn, Fe, and Ti; and (3) the C type shows Ca > Na; Zr >> Nb; minor amounts of Mn, Fe, and Ti.

Combining the information resulting from X-ray diffraction studies and qualitative chemical data, it is possible to conclude that crystals of type A correspond to members of the series låvenite-normandite, whereas types B and C correspond to wöhlerite and hiortdahlite I, respectively.

Electron-Microprobe Analyses

Quantitative chemical analyses were performed using a JEOL JXA-8600 electron-microprobe, operating in wavelength-dispersion mode; the voltage was 15 kV, the beam current was 20 nA, and the beam diameter was set at 5 μm. The following standards were used: titanite (Si$K\alpha$, Ca$K\alpha$, Ti$K\alpha$), albite (Na$K\alpha$), orthoclase (K$K\alpha$, Al$K\alpha$), $MnTiO_3$ (Mn$K\alpha$), FeS_2 (Fe$K\alpha$), diopside (Mg$K\alpha$), monazite (Ce$L\alpha$, Th$M\alpha$, Pr$L\beta$, Sm$L\beta$), La-Re oxide (La$L\alpha$), Nd-Cu alloy (Nd$L\beta$), UO_2 (U$M\alpha$), REE1 (Gd$L\beta$), REE2 (Yb$L\alpha$), REE4 (Dy$L\beta$, Er$L\beta$), zircon (Zr$L\alpha$), yittrium (Y$L\alpha$), metallic niobium (Nb$L\alpha$), metallic tantalum (Ta$M\alpha$), HfO_2 (Hf$M\alpha$), topaz (F$K\alpha$). Corrections were calculated according to the ZAF procedures.

Results of electron-microprobe analyses are reported in Table 2. No quantitative data were collected for the specimen LOS 180, owing to the very small amount of available material.

Låvenite – normandite

According to Perchiazzi *et al.* (2000), the members of the låvenite-normandite series have a chemical composition intermediate between endmembers $NaCaMnTi(Si_2O_7)OF$, corresponding to normandite, and $NaNaMZr(Si_2O_7)F_2$, *i.e.*, låvenite, where *M* is a mixed site hosting Mn, with minor Fe, Ca, and Ti.

The same authors report how sodium and calcium cations filling the mixed *Na* and *Ca* sites are always in excess with respect to the expected value of 2 atoms per formula unit (*apfu*). Moving from "normanditic" to "låvenitic" compositions, the sodium amount increases, according to the mechanism $Na^+ + F^- \rightarrow Ca^{2+} + O^{2-}$, coupled with the substitution $Zr^{4+} \rightarrow Ti^{4+}$ (Fig. 2a). Therefore, a heterovalent substitution $Na^+ + Zr^{4+} + F^- \rightarrow Ca^{2+} + Ti^{4+} + O^{2-}$ can be discussed (Fig. 2b).

TABLE 2. ELECTRON-MICROPROBE ANALYSES OF THE MINERALS OF THE WÖHLERITE GROUP FROM THE LOS ARCHIPELAGO

	låvenite		wöhlerite		hiortdahlite I	
	wt.% (average *n* = 8)	*apfu* (O + F) = 18	wt.% (average *n* = 10)	*apfu* (O + F) = 18	wt.% (average *n* = 19)	*apfu* (O + F) = 18
Nb_2O_5	6.10(23)	0.386	8.28(62)	0.507	1.08(18)	0.063
Ta_2O_5	n.d.		n.d.		n.d.	
SiO_2	26.93(29)	3.772	27.27(17)	3.696	28.36(27)	3.688
TiO_2	4.30(55)	0.453	1.63(21)	0.166	1.17(5)	0.114
ZrO_2	21.70(101)	1.482	13.78(38)	0.911	14.01(44)	0.888
HfO_2	0.36(3)	0.014	0.28(5)	0.011	0.21(4)	0.008
ThO_2	0.03(5)	0.001	0.01(2)	0.000	0.02(3)	0.001
Al_2O_3	n.d.		0.03(5)	0.005	n.d.	
Y_2O_3	0.19(6)	0.014	0.41(10)	0.030	0.58(10)	0.040
La_2O_3	n.d.		0.06(5)	0.003	0.08(5)	0.004
Ce_2O_3	0.06(6)	0.003	0.18(8)	0.009	0.18(7)	0.009
Pr_2O_3	0.04(6)	0.002	0.17(11)	0.008	0.13(9)	0.006
Nd_2O_3	0.03(4)	0.002	0.05(5)	0.002	0.07(6)	0.003
Sm_2O_3	0.12(19)	0.006	0.12(19)	0.006	0.12(18)	0.005
Gd_2O_3	0.09(9)	0.004	0.10(8)	0.004	0.04(7)	0.002
Dy_2O_3	0.07(8)	0.003	0.08(8)	0.003	0.07(10)	0.003
Er_2O_3	0.06(6)	0.003	0.02(5)	0.001	0.05(8)	0.002
Yb_2O_3	0.06(6)	0.003	0.11(10)	0.005	0.10(9)	0.004
CaO	7.74(37)	1.161	27.27(64)	3.960	36.57(54)	5.095
MgO	0.09(1)	0.019	0.59(7)	0.119	0.27(1)	0.052
MnO	11.66(74)	1.383	5.17(22)	0.593	2.66(14)	0.293
FeO	2.48(59)	0.290	1.09(21)	0.124	1.36(20)	0.148
Na_2O	10.59(19)	2.876	6.59(29)	1.732	5.21(28)	1.314
K_2O	n.d.		n.d.		0.01(2)	0.002
F	5.60(35)	2.480	6.48(36)	2.777	10.12(52)	4.162
Sum	98.32(96)		99.77(73)		102.46(85)	
O = F	–2.36		–2.73		–4.26	
Total	95.96		97.04		98.20	

Perchiazzi *et al*. (2000) reported that, moving from normanditic to låvenitic compositions, there is a remarkable drop in the manganese content together with a constant excess of cations filling the *Na*, *Ca*, and (*Zr*,*Ti*) sites. Therefore, in agreement with the above considerations, a full-occupancy for the *Mn* site could be achieved through the double substitution $Mn^{2+} + Ti^{4+} \rightarrow Ca^{2+} + Zr^{4+}$ (Fig. 2c), or with the substitution $Mn^{2+} + Ca^{2+} + F^- \rightarrow Ti^{4+} + Na^+ + O^{2-}$ (Fig. 2d).

The chemical data obtained from the studied specimens indicate that låvenite from the Los Archipelago is enriched in titanium and manganese, in agreement with the previous study of Moreau *et al*. (1996). The chemical formula, recalculated on the basis of 18 anions, is $Na_{2.04}(Ca_{1.12}Na_{0.84}REE_{0.04})(Mn_{1.38}Ti_{0.33}Fe_{0.29}Ca_{0.04}Mg_{0.02})_{\Sigma 2.07}(Zr_{1.48}Nb_{0.38}Ti_{0.13}Hf_{0.01})(Si_{1.89}O_7)_2O_{1.52}F_{2.48}$.

Wöhlerite

The crystal chemical formula of wöhlerite is matter of debate; according to the structural study by Mellini & Merlino (1979), it should be written as $Na_2Ca_4ZrNb(Si_2O_7)_2O_3F$, whereas according to Chakhmouradian *et al*. (2008), it should be written as $Na_2Ca_4(Zr,Nb)_2(Si_2O_7)_2(O,F)_4$, wöhlerite representing the Zr-analogue of marianoite, $Na_2Ca_4(Nb,Zr)_2(Si_2O_7)_2(O,F)_4$.

It could be hypothesized that the substitution of Zr^{4+} by Nb^{5+} could take place through the coupled substitution $Zr^{4+} + F^- \leftrightarrow Nb^{5+} + O^{2-}$. However, no clear relation is observed between zirconium and niobium in the chemical data for wöhlerite (Fig. 3a), suggesting that these two elements do not occupy the same structural position.

Wöhlerite from the Los Archipelago shows the highest manganese content ever measured in this mineral, the average MnO content being 5.17 wt.% (Table 2); the measured fluorine content is also high.

Chemical data for wöhlerite (Figs. 3b,c,d,e) indicate a negative correlation between niobium and fluorine, niobium and manganese, and a positive relationship between manganese and fluorine, suggesting the mecha-

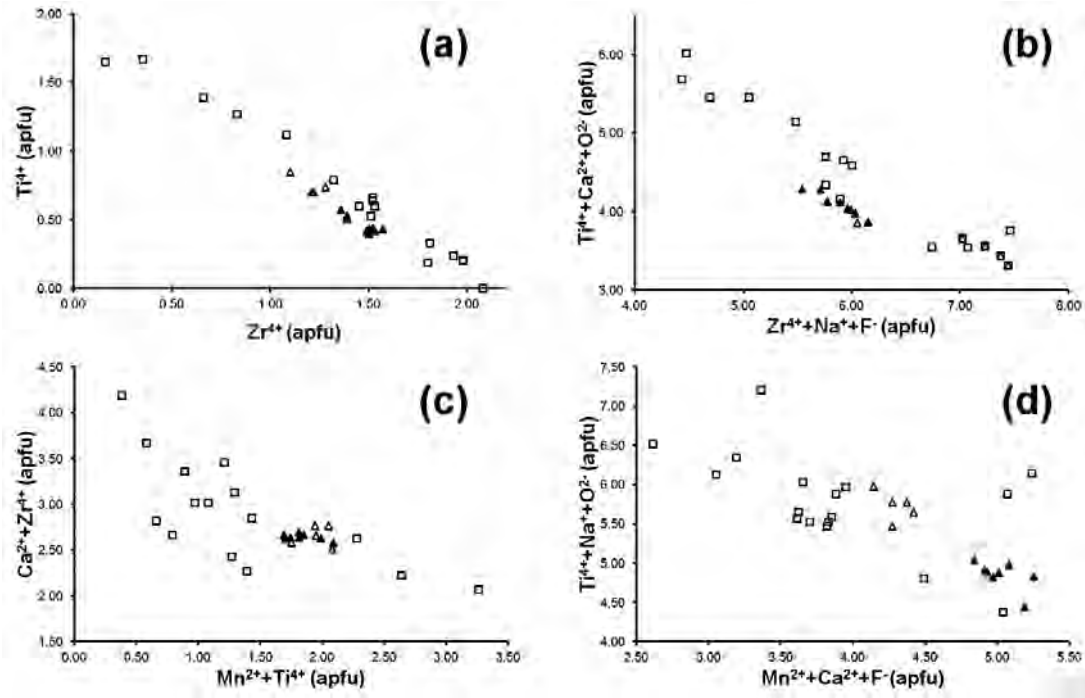

FIG. 2. Chemical relationships (in *apfu*) in the låvenite-normandite series. The empty squares indicate literature data after Mellini (1981) and reference therein, after Chao & Gault (1997), and Perchiazzi *et al*. (2000); empty triangles represent the chemical data of låvenite from Los Archipelago given by Moreau *et al*. (1996). Finally, black triangles show the chemistry of the studied specimens.

nism: $Nb^{5+} + 2Na^{+} + O^{2-} \rightarrow Mn^{2+} + 2Ca^{2+} + F^{-}$, in which manganese could enter into the wöhlerite structure by substituting for some niobium.

The chemical formula of the Mn-rich wöhlerite from the Los Archipelago may be written, following Mellini & Merlino (1979), as $(Na_{1.73}Ca_{0.20}REE_{0.07})(Ca_{3.76}Mn_{0.31}Fe_{0.12})_{\Sigma 4.19}(Zr_{0.92}Mn_{0.08})(Nb_{0.51}Mn_{0.20}Ti_{0.17}Mg_{0.12})(Si_{1.85}O_7)_2O_{1.22}F_{2.78}$.

Hiortdahlite I

According to Merlino & Perchiazzi (1985), the ideal chemical formula of hiortdahlite I is $Na(Na,Ca)Ca_4MZr(Si_2O_7)_2OF_3$, its chemical variability being confined to three sites, indicated as *NaCa*, *M*, and *F*3 in their paper. The substitution $Na^{+} + F^{-} \rightarrow Ca^{2+} + O^{2-}$ describes the variation in occupancy of the mixed *NaCa* site and of the anion *F*3 site. Merlino & Perchiazzi (1985), on the basis of the chemical data of Cleve (Brögger 1890), stated that the average charge for the cations at the *M* site in hiortdahlite I from Langesundsfjord is three, assuming a site occupancy 1/3 Zr^{4+}, 1/6 Ti^{4+}, 1/6 Ca^{2+}, 1/6 Mn^{2+}, 1/6 Fe^{2+}.

The chemical formula for hiortdahlite I from the Los Archipelago, recalculated on the basis of 18 anions, is:

$Na_{1.04}(Ca_{0.66}Na_{0.27}REE_{0.07})Ca_4(Ca_{0.44}Mn_{0.29}Fe_{0.15}Ti_{0.07}Mg_{0.05})(Zr_{0.89}Nb_{0.06}Ti_{0.04}Hf_{0.01})(Si_{3.68}O_{13.84})F_{4.16}$. The *M* site is therefore almost fully occupied by divalent cations (Ca^{2+}, Mn^{2+}, Fe^{2}). Available chemical data for hiortdahlite I point (Fig. 4) to the substitution scheme $Zr^{4+} + Na^{+} + O^{2-} \rightarrow 2(Ca^{2+}, Mn^{2+}, Fe^{2+}) + F^{-}$; the point deviating from the linear relationship represents a specimen of "hiortdahlite" from Tuva (Kapustin & Bykova 1965), whose precise nature is uncertain.

Taking into account the chemical data from the literature for hiortdahlite I from different localities reported in Merlino & Perchiazzi (1985) together with the data given by Robles *et al*. (2001), hiortdahlite I from the Los Archipelago is determined to be the poorest in zirconium and sodium and the richest in calcium and fluorine, and shows one of the highest manganese contents ever recorded in this mineral phase (up to 0.34 Mn *apfu*).

Crystal Structure Refinements

Intensity data collection and crystal structure refinements

The intensity data for the minerals belonging to the wöhlerite group were collected from specimens 106.211, LOS 180, 113.119, and 119.115, corresponding to låvenite, normandite, wöhlerite, and hiortdahlite I, respectively.

Intensity data for låvenite, normandite, and wöhlerite were collected using a Bruker Smart Breeze diffractometer, operating at 50 kV and 30 mA, equipped with an air-cooled CCD area detector, at the Dipartimento di Scienze della Terra, Pisa University. Graphite-monochromated Mo$K\alpha$ radiation was used and the detector-to-crystal working distance was 50 mm. Frames were collected using ϕ and ω scan mode, in 0.5° slices. The number of frames and the exposure time for låvenite, normandite, and wöhlerite were respectively 1634 frames and 10 seconds per frame, 1652 frames and 4 seconds per frame, and 1673 frames with 5 seconds exposure per frame. Intensity data were integrated and corrected for Lorentz, polarization, background effects, and absorption using the APEX2 software package (Bruker AXS Inc., 2004).

The intensity data for hiortdahlite I were collected using a Siemens *P*4 four-circle diffractometer with graphite-monochromated Mo$K\alpha$ radiation at the CIADS (Centro Interdipartimentale di Analisi e Determinazione Strutturale) of Siena University; intensity data were collected in θ-2θ scan mode, scan width 1°, scan

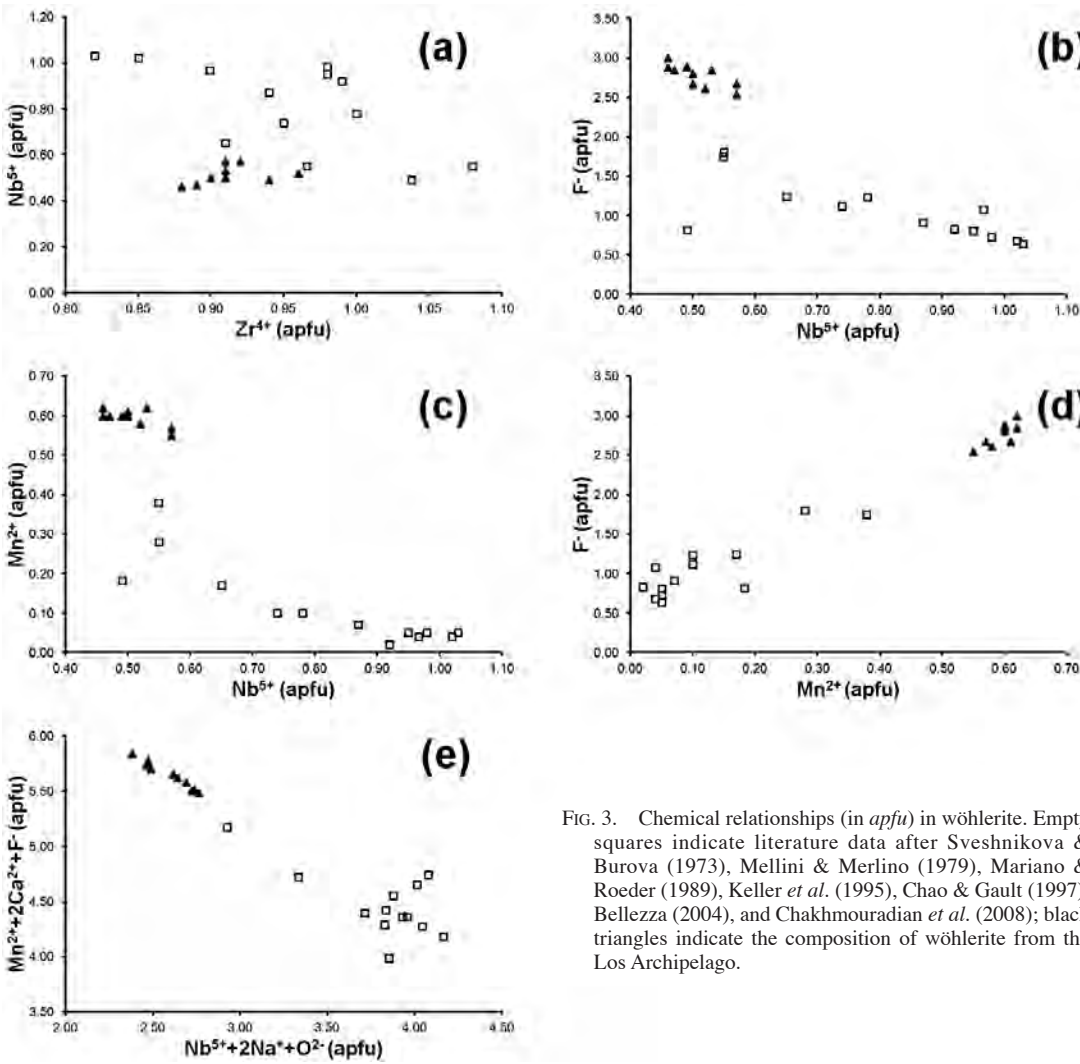

FIG. 3. Chemical relationships (in *apfu*) in wöhlerite. Empty squares indicate literature data after Sveshnikova & Burova (1973), Mellini & Merlino (1979), Mariano & Roeder (1989), Keller *et al*. (1995), Chao & Gault (1997), Bellezza (2004), and Chakhmouradian *et al*. (2008); black triangles indicate the composition of wöhlerite from the Los Archipelago.

speed 2°/min, and corrected for Lorentz-polarization and absorption effect with the ψ-scan method (North *et al.* 1968).

The crystal structures of låvenite, normandite, wöhlerite, and hiortdahlite I were refined using SHELX-97 (Sheldrick 2008), starting from the atomic coordinates given by Mellini (1981), Perchiazzi *et al.* (2000), Mellini & Merlino (1979), and Merlino & Perchiazzi (1985), respectively. Scattering curves for neutral atoms were taken from the International Tables for X-ray Crystallography (1992). Crystal data and details of intensity data collection and refinement are reported in Table 3.

For låvenite, the occupancies of the four cation sites were refined using the following curves: Zr vs Ti for the *Zr* site; Mn vs Ti for the *Mn* site; and Ca vs Na for the *Ca* and *Na* sites. After introducing the anisotropic displacement parameters for the cations, and assuming a normal twinning with twin plane (100), R_1 converged to 0.057, thus validating the initial structural model; the ratio between the twinned domains refined to 0.92(1):0.08(1). In the final steps of the refinement, a mixed O,F occupancy was introduced for the *O*8 site, as suggested by chemical data and by bond-valence balance.

Specimen LOS 180 has a type-I cell; its Ti-rich qualitative composition suggests that it could be normandite. Occupancies of the four cation sites were refined using the same curves used for låvenite. After ten cycles of isotropic refinement, the structure was completed taking into account the anisotropic displacement parameters. The refinement converged to $R_1 = 0.022$, confirming the validity of the structural model.

During the refinement of the crystal structure of wöhlerite, the occupancies of the eight independent cation sites were refined using the following curves: Ca vs □ for the *Ca*1 and *Ca*3 sites; Nb vs Ti for the *Nb* site; Zr vs Mn for the *Zr* site; Ca vs Fe for the *Ca*2 and *Ca*4 sites; and Ca vs Na for the *Ca*5 and *Ca*6 sites. After introducing the anisotropic displacement parameters, R_1 converged to 0.019. In the final steps of the refinement, oxygen atoms were partially substituted by fluorine atoms at sites *O*13, *O*14, and *O*16, as suggested by the bond-valence sum.

For the refinement of hiortdahlite I, the occupancies of the eight independent cation sites were refined using the following curves: Ca vs □ for the *Ca*1, *Ca*2, and *Ca*3 sites; Ca vs Na for the *Ca*4 site; Zr vs Ti for the *Zr* site; Mn vs Ca for the *M* site; Na vs □ for the *Na* site; and Na vs Ca for the *NaCa* site. Assuming isotropic displacement parameters and fixed site-occupancies, ten cycles of refinement converged to $R_1 = 0.20$. After refining the site-scattering values and adding (100) normal twinning, the R_1 value dropped to 0.075. The ratio between the two twinned domains was 0.53(1):0.47(1). Finally, after introducing anisotropic displacement parameters for all the cations, the final R_1 value was 7.3%. In the final steps of the refinement, a partial substitution of oxygen by fluorine at the *O*7 site was introduced, in agreement with the bond-valence balance and chemical data.

Tables of structure factors, cif files and selected bond-distances (Tables S.1 to S.5; see below) are available at the Depository of Unpublished Data of the Mineralogical Association of Canada website [documents Wöhlerite group CM50_593].

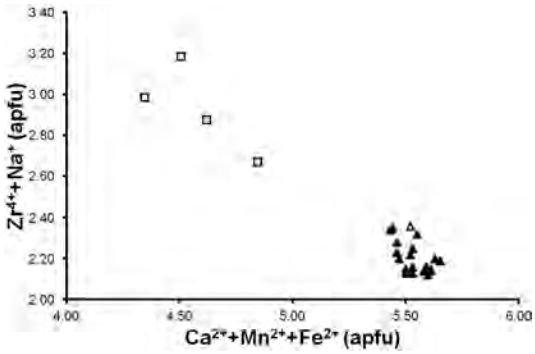

FIG. 4. Chemical relationships between (Zr^{4+}+Na^{+}) *versus* (Ca^{2+} +Mn^{2+}+Fe^{2+}) in hiortdahlite I. The empty squares indicate literature data after Merlino & Perchiazzi (1985) and reference therein; the empty triangle represents the chemical data of hiortdahlite from Los Archipelago given by Robles *et al.* (2001). Finally, black triangles show the chemistry of the studied specimens.

Crystal Structures Details

As previously stated, the crystal structure of the members of the wöhlerite group can be described in modular terms, as composed of disilicate groups and walls of "octahedra".

Selected bond distances for disilicate groups and "octahedral" cations for each refined structure are reported in Tables S.1 and S.2 (deposited).

In agreement with Merlino & Perchiazzi (1988), disilicate groups are always chelated to those polyhedra hosting large-radius and low-charge cations; Si-O bond-lengths and Si-O-Si bond-angles are in good accord with values previously reported in literature.

Table 4 reports the site-scattering values, the proposed site-populations of the walls of "octahedra", and the calculated and observed mean bond-lengths. Site-population assignments are based on the electron-microprobe chemical data. Owing to the absence of quantitative chemical analysis for normandite, the corresponding site-scattering values are not reported in the table. However, they clearly agree with the occupancy of the *Ti* site by titanium and minor zirconium, with a refined site-occupancy of $Ti_{0.72(1)}Zr_{0.28(1)}$, corresponding to 25.6 electrons per formula unit (*epfu*), to be compared with 35.2 *epfu* for låvenite.

TABLE 3. CRYSTAL DATA AND SUMMARY OF PARAMETERS DESCRIBING DATA COLLECTION AND REFINEMENT FOR LÅVENITE, NORMANDITE, WÖHLERITE, AND HIORTDAHLITE I

	låvenite	normandite	wöhlerite	hiortdahlite I
Crystal data				
Crystal size (mm^3)	0.20 × 0.08 × 0.05	0.45 × 0.06 × 0.04	0.17 × 0.10 × 0.04	0.50 × 0.40 × 0.36
Cell setting, space group	Monoclinic, $P2_1/a$	Monoclinic, $P2_1/a$	Monoclinic, $P2_111$	Triclinic, P-1
Unit-cell dimensions				
a (Å)	10.8475(6)	10.8044(7)	10.80498(16)	10.991(7)
b (Å)	9.9364(6)	9.7945(7)	10.25458(13)	10.934(3)
c (Å)	7.1488(4)	7.0532(5)	7.28606(10)	7.366(2)
α (°)				109.60(3)
β (°)	108.392(4)	108.056(3)	109.1168(6)	109.43(2)
γ (°)				83.55(3)
V ($Å^3$)	731.17(7)	709.64(8)	762.78(2)	786.4(6)
Z	2	2	2	2
Data collection and refinement				
Radiation type, (λ)	Mo$K\alpha$ (0.71073 Å)	Mo$K\alpha$ (0.71073 Å)	Mo$K\alpha$ (0.71073 Å)	Mo$K\alpha$ (0.71073 Å)
Temperature (K)	room	room	room	room
Maximum observed 2θ(°)	64.99	65.22	65.17	50.03
Measured reflections	9624	9533	10041	3129
Unique reflections	2665	2625	5265	2664
Reflections $F_o > 4\Sigma F_o$	2301	2369	5013	2360
R_{int}	0.0303	0.0213	0.0141	0.0444
$R\Sigma$	0.0316	0.0195	0.0246	0.0442
Range of h, k, l	$-16 \le h \le 16$ $-14 \le k \le 13$ $-10 \le l \le 10$	$-16 \le h \le 15$ $-14 \le k \le 14$ $-10 \le l \le 10$	$-16 \le h \le 16$ $-15 \le k \le 15$ $-11 \le l \le 9$	$-1 \le h \le 12$ $-12 \le k \le 11$ $-8 \le l \le 8$
R_1 [$F_o > 4\Sigma F_o$]	0.0571	0.0217	0.0192	0.0728
R_1 (all data)	0.0711	0.0265	0.0212	0.0841
wR_2 (on F_o^2)	0.1646	0.0536	0.0458	0.1598
Goof	1.145	1.089	1.028	1.137
Number of l.s. parameters	154	154	280	187
$\Delta\rho_{max}$ and $\Delta\rho_{min}$	2.94, –1.19	1.07, –0.99	0.83, –1.05	1.07, –1.36

Låvenite and normandite have four independent "octahedral" sites (Figs. 5a and 5b). The *Na* and *Ca* sites host sodium and calcium cations. The *Mn* site has a mixed occupancy by manganese with minor titanium, iron, and probably calcium. Finally, the *Zr* (in låvenite) and *Ti* (in normandite) sites have a mixed Zr/Ti occupancy, with Zr > Ti in the former and Ti > Zr in the latter. The greater the Ti content, the smaller the average bond-length, changing from 2.07 Å in the Zr-centered octahedron to 2.00 Å in the Ti-centered octahedron. Analogously, the distortion of this polyhedron increases from låvenite to normandite, owing to the off-center displacement (Megaw 1968) related to the occurrence of the small-radius and high-charge Ti^{4+} cation. According to Subbotin *et al.* (2000), zirconium and titanium may play a different crystal chemical role owing to their different effective charge, giving rise to a quite limited isostructurality between Zr- and Ti-analogues. In agreement with this observation, for example, no correlation between Zr^{4+} and Ti^{4+} was observed in Zr-rich cuspidine from Pian di Celle, Umbria, Italy (Bellezza *et al.* 2004b). On the contrary, taking into account the series låvenite-normandite, a negative correlation between Zr and Ti is clearly discernible (Fig. 2a). One possible explanation to this apparently conflicting behavior comes from the observation of definitely higher manganese content in normandite with respect to låvenite. We would also remark that the only other member of the wöhlerite group with titanium as the dominant cation at small octahedral sites is janhaugite, which contains a significant amount of manganese, with three independent *Mn* sites in its structure. In this perspective, in the normandite structure the edge of a Ti-centered polyhedron would comfortably fit the edge of a Mn-centered

octahedron in an adjacent column, whereas in the låvenite structure, or when a Zr/Ti substitution happens in normandite, a larger Ca-centered polyhedron would instead fit with the edge of a larger Zr octahedron hosted in an adjacent column.

Wöhlerite has eight independent cation sites, owing to their non-centrosymmetric distribution in the walls of "octahedra" (Fig. 5c). Taking into account the refined site-scattering factor and the geometrical features (Table 4), the sites hosting large-radius and small-charge cations, like calcium and sodium, do not show significant differences from those described by Mellini & Merlino (1979) for wöhlerite; in the same way, the *Zr* site has only a slightly lower electron-density, compatible with a minor substitution by a lighter cation. In addition, the Zr-centered octahedron is a nearly regular polyhedron, with five short bonds (average bond-length 2.060 Å) and a longer bond (2.173 Å), quite similar to the *Zr* polyhedron of wöhlerite described by Mellini & Merlino (1979) and the *M*2 octahedron of marianoite (Chakhmouradian *et al*. 2008). On the contrary, the *Nb* site shows (Table 4) a refined site-scattering definitely lower than the expected value, indicating a significant substitution of niobium by lighter cations. Moreover, the geometry of the Nb-centered octahedron of the Mn-rich wöhlerite from the Los Archipelago is rather different from the *Nb* polyhedron in wöhlerite and the *M*1 polyhedron in marianoite. In fact, whereas the Nb-centered octahedron of wöhlerite from Brevig (Mellini & Merlino 1979) and the *M*1 polyhedron of marianoite (Chakhmouradian *et al*. 2008) have average bond distances of 2.033 Å and 2.031 Å respectively, the Nb octahedron of the wöhlerite from Los Archipelago is larger, with an average bond length of 2.073 Å (see Supplementary Table S.2). These data point to the substitution of the small radius Nb^{5+} cations by lighter and larger ones, such as Mn^{2+} and Mg^{2+}. Full occupancy of *Nb* site was achieved by introducing all the titanium at this site, given its similar off-centre displacement effect. The remaining available manganese was added to the *Zr* site, achieving the full occupancy of this site.

Hiortdahlite I has eight independent cation sites, located in two structurally different "walls" (Fig. 6a), a first "wall" being formed by *Ca*1, *Zr*, *Ca*4, and *Na* polyhedra (Fig. 6b), and a second one hosting *Ca*, *Ca*3, *NaCa*, and *M* polyhedra (Fig. 6c). Comparing hiortdahlite I from the Los Archipelago with hiortdahlite I from Langesundsfjord, Norway, as described by Merlino & Perchiazzi (1985), it is apparent that the most relevant difference is related to the site-occupancy of the *M* octahedron. Refined site-scattering factors and electron-microprobe analysis point to a site-occupancy

TABLE 4. REFINED SITE-SCATTERING VALUES (*epfu*) AND ASSIGNED SITE-POPULATION (*apfu*) FOR CATION SITES IN LÅVENITE, WÖHLERITE, AND HIORTDAHLITE I

Site	Site-scattering	Site-population*	Calculated site-scattering	$\langle X\text{-}\phi\rangle_{calc}$* Å	$\langle X\text{-}\phi\rangle_{obs}$ Å
låvenite					
Zr	35.2	$Zr_{0.74}Nb_{0.19}Ti_{0.07}$	38.9	2.07	2.07
Mn	24.4	$Mn_{0.67}Ti_{0.16}Fe_{0.14}Ca_{0.02}Mg_{0.01}$	24.4	2.14	2.22
Ca	16.4	$Ca_{0.58}Na_{0.42}$	16.2	2.50	2.53
Na	13.0	$Na_{1.00}$	11.0	2.52	2.57
wöhlerite					
*Ca*1	19.8	$Ca_{1.00}$	20.0	2.49	2.52
Nb	30.8	$Nb_{0.51}Mn_{0.20}$ $Ti_{0.17}Mg_{0.12}$	31.1	2.05	2.07
Zr	38.2	$Zr_{0.92}Mn_{0.08}$	38.8	2.10	2.08
*Ca*2	22.2	$Ca_{0.64}Mn_{0.26}Fe_{0.10}$	21.9	2.32	2.31
*Ca*3	19.7	$Ca_{1.00}$	20.0	2.43	2.43
*Ca*4	20.2	$Ca_{1.00}$	20.0	2.37	2.37
*Na*1	12.6	$Na_{0.80}Ca_{0.20}$	12.8	2.51	2.56
*Na*2	11.8	$Na_{0.90}Ca_{0.10}$	11.9	2.52	2.58
hiortdahlite I					
*Ca*1	19.8	$Ca_{1.00}$	20.0	2.49	2.50
*Ca*2	19.8	$Ca_{1.00}$	20.0	2.37	2.36
*Ca*3	21.7	$Ca_{1.00}$	20.0	2.37	2.34
*Ca*4	18.4	$Ca_{1.00}$	20.0	2.42	2.43
Zr	36.0	$Zr_{0.90}Nb_{0.05}Ti_{0.05}$	39.2	2.08	2.11
M	23.4	$Ca_{0.44}Mn_{0.29}Fe_{0.15}Ti_{0.07}Mg_{0.05}$	22.1	2.23	2.26
Na	13.5	$Na_{0.95}REE_{0.05}$	13.0[1]	2.48[2]	2.51
NaCa	15.5	$Ca_{0.65}Na_{0.35}$	16.8	2.49	2.54

* Ionic radii from Shannon & Prewitt, 1969; [1] mean scattering curve of 49.94 for Y^{3+} and REE^{3+}; [2] ionic radius of $^{[VII]}Na^{+}$

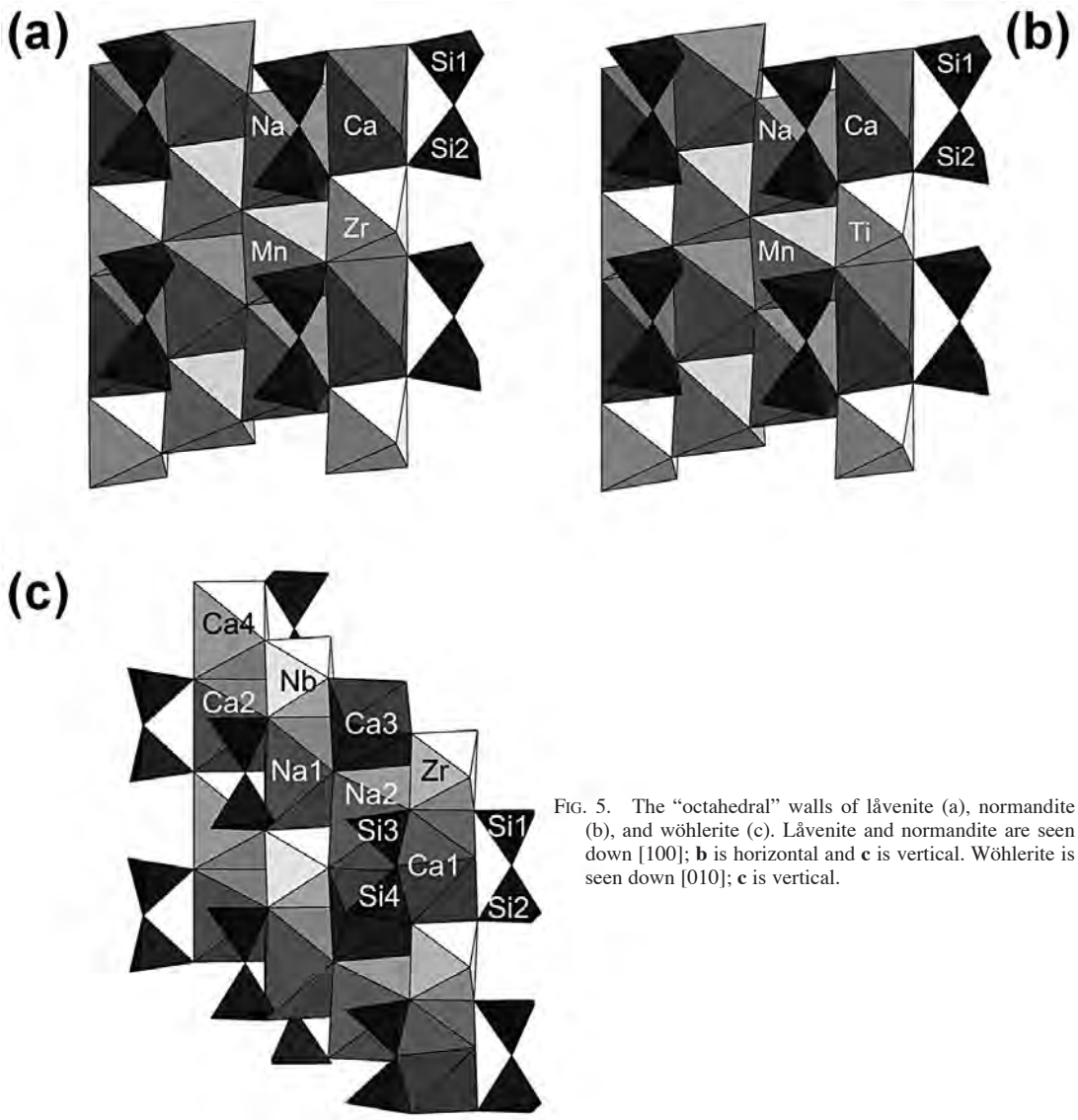

FIG. 5. The "octahedral" walls of låvenite (a), normandite (b), and wöhlerite (c). Låvenite and normandite are seen down [100]; **b** is horizontal and **c** is vertical. Wöhlerite is seen down [010]; **c** is vertical.

by calcium, manganese, iron, with minor titanium and magnesium, with an average charge of 2.14, compared with the average charge of 3 for hiortdahlite I from Norway (Merlino & Perchiazzi, 1985); the lower charge of the *M* site is in agreement with the high fluorine content of hiortdahlite I from the Los Archipelago.

The site-occupancy of anions in the refined crystal structures (reported in Tables S.3, S.4, and S.5, deposited) was inferred on the basis on bond-valence sums, in agreement with Brese & O'Keeffe (1991).

In the crystal structures of låvenite and normandite nine independent anion sites are present. The bond-valence balance (Table S.3) suggest that *O*1-*O*7 sites are occupied by oxygen, whereas *F*9 is a fluorine-bearing site. *O*8 is a mixed O,F site in låvenite, in agreement with Mellini (1981), whereas it is fully occupied by oxygen in normandite.

Eighteen independent anion sites occur in the crystal structures of wöhlerite and hiortdahlite I. In wöhlerite from the Los Archipelago (Table S.4), *O*1 to *O*12 and *O*17 and *O*18 are pure oxygen sites, and the full occupancy of *F*15 by fluorine is confirmed. The *O*13, *O*14, and *O*16 sites are undersatured, suggesting a mixed O,F occupancy, in agreement with electron-microprobe data.

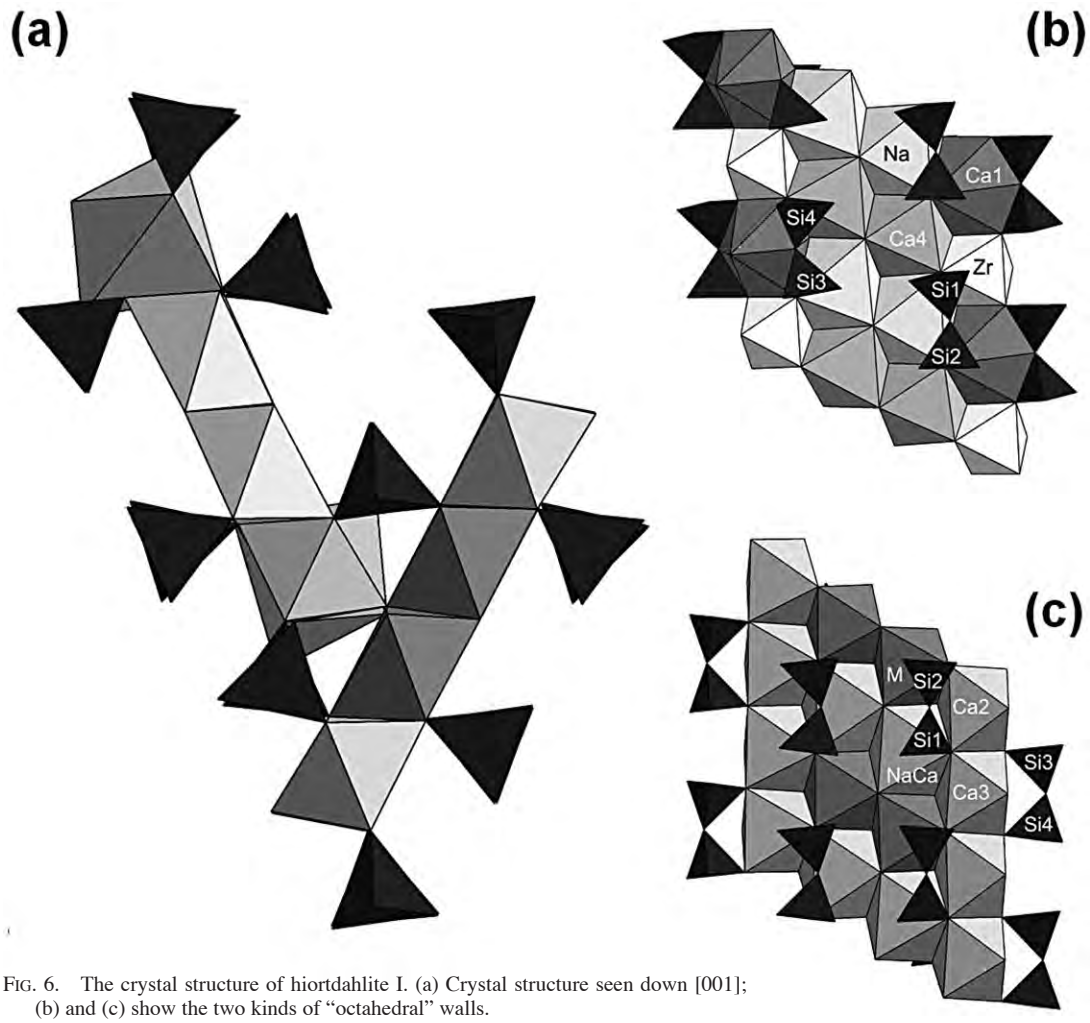

FIG. 6. The crystal structure of hiortdahlite I. (a) Crystal structure seen down [001]; (b) and (c) show the two kinds of "octahedral" walls.

It is noteworthy that these three latter sites are bonded to the Nb-centered octahedron, in which manganese partially substitutes for niobium, through the scheme $Nb^{5+} + 2Na^{+} + O^{2-} \rightarrow Mn^{2+} + 2Ca^{2+} + F^{-}$ (Fig. 3d). In the refined hiortdahlite I structure from the Los Archipelago, bond-valence calculation (Table S.5) indicate a full oxygen occupancy of *O*1 to *O*6 and *O*8 to *O*15 sites, a full fluorine occupancy at *F*1, *F*2, and *F*3 sites, and a mixed occupancy by oxygen and fluorine at the *O*7 site.

Partitioning of zirconium and niobium in wöhlerite

The results obtained during the refinement of the crystal structure of Mn-rich wöhlerite from the Los Archipelago allow us to draw some conclusions about the different crystal chemical behavior of niobium and zirconium in wöhlerite.

As previously reported, Mellini & Merlino (1979) and Chakhmouradian *et al.* (2008) proposed two different crystal-chemical formulae for wöhlerite, $Na_2Ca_4ZrNb(Si_2O_7)_2O_3F$ or $Na_2Ca_4(Zr,Nb)_2(Si_2O_7)_2O_3F$, respectively. The difference is related to the possible ordering of (Nb+Ti) and Zr at the two smallest octahedrally coordinated sites. Owing to the very similar X-ray scattering factors, the ratio of zirconium and niobium at these sites cannot be refined directly using radiation routinely employed in laboratory equipment, such as Mo$K\alpha$. According to Mellini & Merlino (1979), the distinct occupancy of these two sites is suggested by: (1) their different size, (2) their different distortion, and (3) their different equivalent thermal parameters. Chakhmouradian *et al.* (2008) criticized these arguments, stating that there is no convincing empirical evidence for the ordering of niobium and zirconium at two distinct sites

and that the extensive substitutions in different members of the wöhlerite group attest to a great structural flexibility of these phases. Therefore, according to these latter authors, wöhlerite would contain zirconium dominant at both sites, whereas marianoite would contain niobium dominant at both sites.

The structural data for Mn-rich wöhlerite presented in this study can be examined to obtain evidence supporting one of these two contrasting interpretations. As the geometry of a coordination polyhedron is controlled by several parameters, both intrinsic (*e.g.*, the site occupancy) and extrinsic (*i.e.*, the electrostatic forces exerted by ions outside the nearest coordination sphere), it is particularly interesting to compare polyhedra in the crystal structure of the same mineral group.

The size and the degree of distortion of the small octahedra, preferentially occupied by zirconium, niobium, and titanium in the minerals of the wöhlerite group, can be evaluated through the comparison of some parameters, reported in Table 5 together with the site occupancies of the above-mentioned small octahedra. Merlino & Mellini (2009) used the parameter Δ as an indication of the degree of distortion. According to Robinson *et al.* (1971), the measure of the distortion of coordination polyhedra can be also expressed through two parameters, namely the bond angles variance (Σ^2) and the mean quadratic elongation (λ). For a coordination octahedron, $\Sigma^2 = (1/11)\ \Sigma\ (\theta_i\text{-}90°)^2$ and $\lambda = (1/6)\ \Sigma\ (l_i/l_0)^2$, where θ_i are the bond angles, l_i are the bond-lengths, and l_0 is the bond-length for the ideal undistorted octahedron equal in volume to the one in question. Figures 7, 8a, and 8b illustrate the relation between the zirconium content and some geometrical parameters, such as the average bond-length, the polyhedron volume, the octahedral angle variance Σ^2, the mean octahedral quadratic elongation λ, and the Δ parameter. One can notice that the Zr-dominant sites clearly form a distinct group, with longer average bond-lengths, greater polyhedron volumes, and lower Δ, Σ^2, and λ values. The only exception is represented by the Zr-centered octahedron of baghdadite, which has higher values of both Σ^2 and λ. These geometric features, shown also by the synthetic counterpart studied by Plaisier *et al.* (1995), are probably induced by the unusual cation distribution in its walls of "octahedra", with two Zr polyhedra connected through edge-sharing. The (Nb,Ti)-dominant sites constitute, on the other hand, a group with significantly shorter bond-lengths, smaller polyhedron volumes, and greater Σ^2, λ, and Δ values. The *Nb* site in wöhlerite from the Los Archipelago represents an exception, owing to its high manganese content. Marianoite was not reported in these plots, because Chakhmouradian *et al.* (2008) did not report the site occupancies of the two small octahedral sites *M*1 and *M*2. In Figure 8c the relations between two geometrical features, namely Σ^2 and λ, are

TABLE 5. GEOMETRICAL PARAMETERS OF NB, TI, AND ZR SITES IN MINERALS BELONGING TO THE WÖHLERITE GROUP

	Site	Site occupancy	average bond-length (Å)	average edge-length (Å)	average angle (°)	polyhedral volume (Å^3)	Σ^2	λ	Δ	Ref.
baghdadite	*Zr*	$Zr_{0.86}Ti_{0.14}$	2.104	2.961	105.84	11.962	82.61	1.026	0.23	[1]
burpalite	*Zr*	Zr	2.097	2.962	107.06	12.196	17.89	1.005	0.04	[2]
hiortdahlite I	*Zr*	Zr	2.089	2.951	106.94	12.031	23.00	1.008	0.18	[3]
hiortdahlite I	*Zr*	$Zr_{0.90}\ Nb_{0.05}Ti_{0.05}$	2.110	2.979	106.74	12.352	29.03	1.010	0.19	[4]
hiortdahlite II	*Zr*	Zr	2.149	3.035	106.89	13.080	25.28	1.008	0.09	[5]
janhaugite	*Ti*1	$Ti_{0.7}Zr_{0.3}$	2.015	2.842	105.95	10.736	37.15	1.014	0.37	[6]
	*Ti*2	$Ti_{0.7}Zr_{0.3}$	2.010	2.832	105.53	10.608	45.68	1.019	0.44	
låvenite	*Zr*	$Zr_{0.86}Nb_{0.14}$	2.083	2.941	106.49	11.910	25.22	1.009	0.21	[7]
låvenite	*Zr*	$Zr_{0.74}Nb_{0.17}Ti_{0.09}$	2.069	2.922	106.53	11.691	24.06	1.009	0.25	[4]
marianoite	*M*1		2.031	2.858	105.64	10.962	44.07	1.019	0.44	[8]
	*M*2		2.080	2.938	106.86	11.884	22.13	1.007	0.10	
niocalite	*Nb*	Nb	2.049	2.884	105.67	11.180	60.08	1.022	0.37	[9]
normandite AF	*Ti*	$Ti_{0.61}Zr_{0.39}$	2.028	2.860	106.06	10.962	34.02	1.014	0.41	[10]
normandite MSH	*Ti*	$Ti_{0.88}Nb_{0.12}$	2.003	2.821	105.80	10.534	39.50	1.018	0.52	[10]
normandite	*Ti*	$Ti_{0.75}Zr_{0.25}$	2.000	2.818	105.81	10.497	38.55	1.017	0.51	[4]
wöhlerite	*Nb*	$Nb_{0.8}Ti_{0.2}$	2.034	2.865	105.83	11.031	39.65	1.017	0.42	[11]
	Zr	Zr	2.083	2.944	107.02	11.965	17.43	1.005	0.12	
wöhlerite	*Nb*	$Nb_{0.51}Mn_{0.20}$ $Ti_{0.17}Mg_{0.12}$	2.073	2.922	106.47	11.667	36.77	1.014	0.34	[4]
	Zr	$Zr_{0.92}Mn_{0.08}$	2.078	2.934	106.97	11.848	18.36	1.006	0.14	

[1] Biagioni *et al.* (2010b); [2] Merlino *et al.* (1990); [3] Merlino & Perchiazzi (1985); [4] this work; [5] Merlino & Perchiazzi (1987); [6] Annehed *et al.* 1985; [7] Mellini (1981); [8] Chakhmouradian *et al.* (2008); [9] Mellini (1982); [10] Perchiazzi *et al.* (2000); [11] Mellini & Merlino (1979).

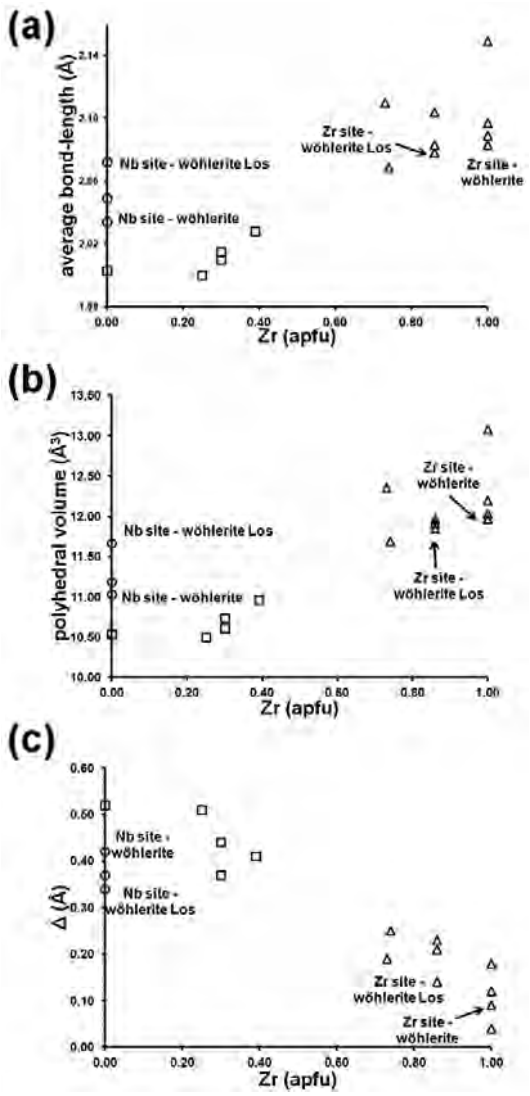

FIG. 7. Relationships between the site occupancy of the small octahedral sites and the average bond-length (a), polyhedral volume (b), and Δ parameter (c) in minerals of the wöhlerite group. Circles: Nb sites; square: Ti sites; triangles: Zr sites.

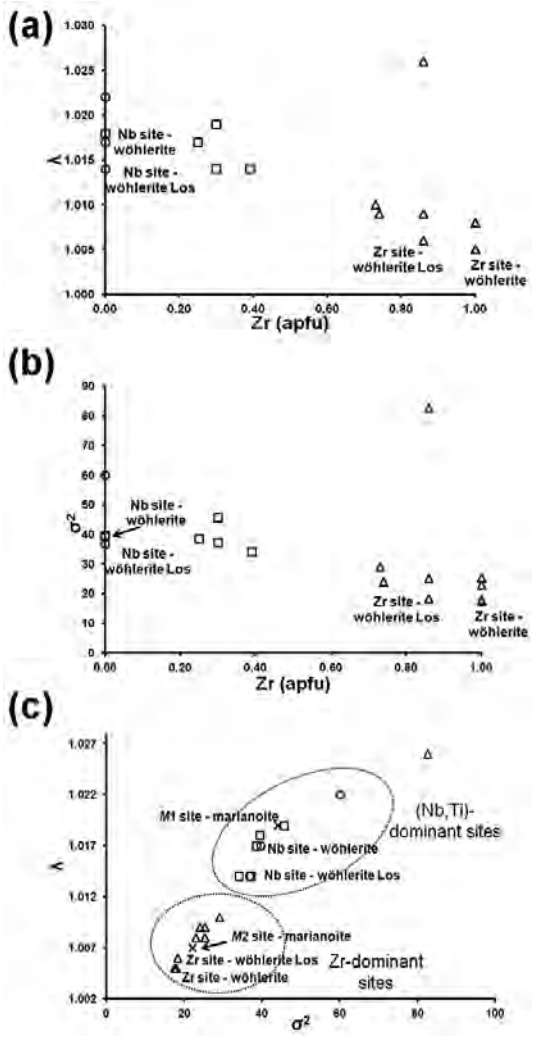

FIG. 8. Relationships between the site occupancy of the small octahedral sites and their octahedral angle variance Σ^2 (a) and mean octahedral quadratic elongation λ (b). In (c), these two geometric parameters are compared. Circles: Nb sites; square: Ti sites; triangles: Zr sites. In (c), crosses indicate the two small octahedral sites of marianoite.

shown: two distinct groups can be identified, *i.e.*, one group including the Zr-dominant sites, and the other comprising the (Nb,Ti)-dominant sites. It is interesting to note that the *M*2 and the *M*1 sites of marianoite fall within the former and the latter groups, respectively. Figure 8c therefore suggests that, in the wöhlerite group, (*Nb*,*Ti*) and *Zr* sites can be distinguished on the basis of geometrical parameters. In the light of these data, marianoite could be considered a wöhlerite with *M*1 and *M*2 sites dominated by niobium and zirconium, respectively. As suggested by Merlino & Mellini (2009), studies through anomalous scattering, with synchrotron X-ray radiation of appropriate wavelength, would allow direct investigation of the Zr/Nb distribution in the octahedral sites of wöhlerite and marianoite.

Conclusions

Coupling X-ray diffraction and chemical data, four different phases belonging to the wöhlerite group were identified in the nepheline syenites from the Los Archipelago: låvenite, normandite, wöhlerite, and hiortdahlite I. In the light of our data, the occurrence of hiortdahlite II, described by Robles *et al*. (2001) appears quite doubtful.

A chemical feature common to all the investigated minerals of the wöhlerite group is their quite high manganese content, this being the highest ever measured in wöhlerite. The wide range of Zr/Ti ratio in the låvenite-normandite series, not detected in other mineral series, could be explained through the coupled substitution of manganese by calcium. Normandite could host contemporaneously Ti- and Mn-centered octahedra in adjacent columns, bonded through edge-sharing, both smaller in size with respect to Zr- and Ca-octahedra occurring in the crystal structure of låvenite. The comparison of the geometry of the (Nb,Ti)- and Zr-centered polyhedra, including all available structural studies of the wöhlerite group, indicates that a distinction is possible between (Nb,Ti)- and Zr-dominant sites in this mineral family.

The results from the present study and the recent discovery of the new mineral roumaite (Biagioni *et al*., 2010a) in the nepheline syenites from the Los Archipelago suggests that, taking into account the richness in mineral species of other famous alkaline complexes, *i.e*., more than 400 different mineral species reported in the Mont Saint-Hilaire, Khibiny, and Lovozero massifs, further sampling and lab studies will possibly greatly increase the number of mineral species described from this locality.

Acknowledgments

For this research, we received support from the SYNTHESYS Project (FR-TAF-2137: "Crystallography and crystal chemistry of rare Zr-Ti-Nb phases from Iles de Los, Guinea"; http://www.synthesys.info/), which is financed by the European Community Research Infrastructure Action under the FP6 "Structure the European Research Area" and by MIUR through project PRIN 2007 "Compositional and structural complexity in minerals (crystal chemistry, microstructures, modularity, modulations): analysis and applications". We are grateful to Editor Robert F. Martin, to Associated Editor Ian Coulson, to Fernando Cámara and to an anonymous referee for the comments and suggestions that helped us in improving the manuscript.

References

Annehed, H., Falth, L., & Raade, G. (1985) The crystal structure of janhaugite, a sorosilicate of the cuspidine family. *Neues Jahrbuch für Mineralogie (Monatshefte)* **1985**, 7-18.

Atencio, D., Coutinho, J.M.V., Ulbrich, M.N.C., Vlach, S.R.F., Rastsvetaeva, R.K., & Pushcharovksy, D.Y. (1999) Hainite from Poços de Caldas, Minas Gerais, Brazil. *Canadian Mineralogist*, **37**, 91-98.

Bellezza, M. (2004) *Studio cristallochimico di Zr,Ti,Nb,REE-disilicati con formula generale* $M_{16}(Si_2O_7)_4(O,OH,F)_8$ *appartenenti alle famiglie di cuspidina, götzenite-rosenbuschite-seidozerite e rinkite*. Ph.D. Thesis, Università di Pisa, 219pp.

Bellezza, M., Franzini, M., Larsen, A.O., Merlino, S., & Perchiazzi, N. (2004a) Grenmarite, a new member of the götzenite-seidozerite-rosenbuschite group from the Langesundsfjord distict, Norway: definition and crystal structure. *European Journal of Mineralogy* **16**, 971-978.

Bellezza, M., Merlino, S., & Perchiazzi, N. (2004b) Chemical and structural study of the Zr,Ti-disilicates in the venanzite from Pian di Celle, Umbria, Italy. *European Journal of Mineralogy* **16**, 957-969.

Bellezza, M., Merlino, S., & Perchiazzi, N. (2009) Mosandrite: structural and crystal-chemical relationship with rinkite. *Canadian Mineralogist* **47**, 897-908.

Biagioni, C., Bonaccorsi, E., Merlino, S., Parodi, G.C., Perchiazzi, N., Chevrier, V., & Bersani, D. (2010a) Roumaite, $(Ca,Na,\square)_3(Ca,REE,Na)_4(Nb,Ti)[Si_2O_7]_2(OH)F_3$, from Rouma Island, Los Archipelago, Guinea: a new mineral species related to dovyrenite. *Canadian Mineralogist* **48**, 17-28.

Biagioni, C., Bonaccorsi, E., Perchiazzi, N., & Merlino, S. (2010b) Single crystal refinement of the structure of baghdadite from Fuka (Okayama Prefecture, Japan). *Periodico di Mineralogia* **79**, 1-9.

Brese, N.E. & O'Keeffe, M. (1991) Bond-valence parameters for solids. *Acta Crystallographica* **B47**, 192-197.

Brögger, W.C. (1890) Die Mineralien der Syenitpegmatitgänge der Südnorwegischen Augit- und Nephelinsyenite. Hiortdahlit. *Zeitschrift für Kristallographie und Mineralogie* **16**, 367-377.

Bruker AXS Inc. (2004) APEX 2. Bruker Advanced X-ray Solutions, Madison, Wisconsin, USA.

Cámara, F., Sokolova, E., & Hawthorne, F. (2011) From structure topology to chemical composition. XII. Titanium silicates: the crystal chemistry of rinkite, Na_2Ca_4*REE*$Ti(Si_2O_7)_2OF_3$. *Mineralogical Magazine* **75**, 2755-2774.

Chakhmouradian, A.R., Mitchell, R.H., Burns, P.C., Mikhailova, Yu., & Reguir, E.P. (2008) Marianoite, a new member of the cuspidine group from the Prairie Lake silicocarbonatite, Ontario. *Canadian Mineralogist* **46**, 1023-1032.

CHAO, G.Y. & GAULT, R.A. (1997) Normandite, the Ti-analogue of låvenite from Mount Saint-Hilarie, Québec. *Canadian Mineralogist* **35**, 1035-1039.

CHRISTIANSEN, C.C., GAULT, R., GRICE, J.D., & JOHNSEN, O. (2003a) Kochite, a new member of the rosenbuschite group from the Werner Bjerge alkaline complex, East Greenland. *European Journal of Mineralogy* **15**, 551-554.

CHRISTIANSEN, C.C., JOHNSEN, O., & MAKOVICKY, E. (2003b) Crystal chemistry of the rosenbuschite group. *Canadian Mineralogist* **41**, 1203-1224.

COULSON, I.M. (1997) Post-magmatic alteration in eudialyte from the North Qôroq centre, South Greenland. *Mineralogical Magazine* **61**, 99-109.

FERGUSON, A.K. (1978) The occurrence of ramsayite, titan-låvenite and a fluorine-rich eucolite in a nepheline-syenite inclusion from Tenerife, Canary Island. *Contributions to Mineralogy and Petrology* **66**, 15-20.

HENTSCHEL, G. (1986) Neue mineralfunde aus quartären vulkanvorkommen der Eifel. *Mainzer Geowissenschaftliche Mitteilungen* **15**, 215-218.

HORVÁTH, L. & GAULT, R.A. (1990) The mineralogy of Mont Saint-Hilaire (Quebec). *Mineralogical Record* **21**, 284-359.

HORVÁTH, L., PFENNINGER-HORVÁTH, E., GAULT, R., & TARASSOFF, P. (1998) Mineralogy of the Saint-Amable sill (Varennes and Saint-Amable, Quebec). *Mineralogical Record* **29**, 83-116.

INTERNATIONAL TABLES FOR X-RAY CRYSTALLOGRAPHY (1992) Volume C. Kluwer Academic Publishers, Dordrecht, The Netherlands.

KADIYSKI, M., ARMBRUSTER, T., GAŁUSKIN, E.V., PERTSEV, N.N., ZADOV, A.E., GAŁUSKINA, I.O., WRZALIK, R., DZIERŻANOWSKI, P., & KISLOV, E.V. (2008) The modular structure of dovyrenite, $Ca_6Zr[Si_2O_7]_2(OH)_4$: alternate stacking of tobermorite and rosenbuschite-like units. *American Mineralogist* **93**, 456-462.

KAPUSTIN, Y. & BYKOVA, A.V. (1965) First find of hiortdahlite in the USSR. *Doklady Akademii Nauk SSSR*, **161**, 121-124.

KELLER, J., WILLIAMS, C.T., & KOBERSKI, U. (1995) Niocalite and wöhlerite from the alkaline and carbonatite rocks at Kaiserstuhl, Germany. *Mineralogical Magazine* **59**, 561-566.

LACROIX, A. (1908) Sur l'existence du fluorure de sodium cristallisé comme element des syénites néphéliniques des îles de Los. *Comptes Rendus de l'Académie des Sciences Paris* **146**, 213-216.

LACROIX, A. (1911) Les syénites néphéliniques de l'archipel de Los et leurs minéraux. *Nouvelles Archives du Muséum d'Histoire Naturelle* **3**, 1-132.

LACROIX, A. (1924) Nouvelles observations sur les syénites néphéliniques des Iles de Los (Guinée). *Comptes Rendus de l'Académie des Sciences Paris* **178**, 1109-1114.

LACROIX, A. (1931) Les pegmatites de la syénite sodalitique de l'île Rouma (archipel de Los, Guinée française). Description d'un noveau minéral (sérandite) qu'elles renferment. *Comptes Rendus de l'Académie des Sciences Paris* **192**, 189-194.

LAZARENKOV, V.G. (1975) *Feldspathoid syenites, Los massif (Guinea)*. Izdatelistvo Leningradskogo Universiteta, 147 pp.

MARIANO, A.N. & ROEDER, P.L. (1989) Wöhlerite: chemical composition, cathodoluminescence and environment of crystallization. *Canadian Mineralogist* **27**, 709-720.

MEGAW, H.D. (1968) A simple theory of the off centre displacement of cations in octahedral environments. *Acta Crystallographica* **B24**, 149-153.

MELLINI, M. (1981) Refinement of the crystal structure of låvenite. *Tschermaks Mineralogische Petrographische Mitteilungen* **28**, 99-112.

MELLINI, M. (1982) Niocalite revised: twinning and crystal structure. *Tschermaks Mineralogische Petrographische Mitteilungen* **30**, 249-266.

MELLINI, M. & MERLINO, S. (1979) Refinement of the crystal structure of wöhlerite. *Tschermaks Mineralogische Petrographische Mitteilungen* **26**, 109-123.

MERLINO, S., BONACCORSI, E., & ARMBRUSTER, T. (1999) Tobermorites: their real structure and order-disorder (OD) character. *American Mineralogist* **84**, 1613-1621.

MERLINO, S. & MELLINI, M. (2009) Marianoite, a new member of the cuspidine group from the Prairie Lake silicocarbonatite, Ontario: discussion. *Canadian Mineralogist* **47**, 1275-1279.

MERLINO, S. & PERCHIAZZI, N. (1985) The crystal structure of hiortdahlite I. *Tschermaks Mineralogische Petrographische Mitteilungen* **34**, 297-310.

MERLINO, S. & PERCHIAZZI, N. (1987) The crystal structure of hiortdahlite II. *Mineralogy and Petrology* **37**, 25-35.

MERLINO, S. & PERCHIAZZI, N. (1988) Modular mineralogy in the cuspidine group of minerals. *Canadian Mineralogist* **26**, 933-943.

MERLINO, S., PERCHIAZZI, N., KHOMYAKHOV, A.P., PUSHCHAROVSKII, D.Y., KULIKOVA, I.M., & KUZMIN, V.I. (1990) Burpalite, a new mineral from Burpalinskii massif, North Transbajkal, USSR: its crystal structure and OD character. *European Journal of Mineralogy* **2**, 177-185.

MOREAU, C., OHNESTETTER, D., DEMAIFFE, D., & ROBINEAU, B. (1996) The Los Archipelago nepheline syenite ring-structure: a magmatic marker of the evolution of the central and equatorial Atlantic. *Canadian Mineralogist* **34**, 281-299.

NORTH, A.C.T., PHILLIPS, D.C., & MATHEWS, F.S. (1968) A semi-empirical method of absorption correction. *Acta Crystallographica* **A24**, 351-359.

PARODI, G.C. & CHEVRIER, V. (2004) New discoveries in nephelinites from Los Island (Republic of Guinea). 5th International Conference "Mineralogy and Museum", Paris. *Bulletin de la Société Française de Minéralogie et de Cristallographie* **16**.

PERCHIAZZI, N., MCDONALD, A.M., GAULT, R.A., JOHNSEN, O., & MERLINO, S. (2000) The crystal structure of normandite and its crystal-chemical relationship with låvenite. *Canadian Mineralogist* **38**, 641-648.

PLAISIER, J.R., JANSEN, J., DE GRAAF, R.A.G., & IJDO, D.J.W. (1995) Structure determination of $Ca_3HfSi_2O_9$ and $Ca_3ZrSi_2O_9$ from powder diffraction. *Journal of Solid State Chemistry* **115**, 464-468.

RIDOLFI, F., RENZULLI, A., SANTI, P., & UPTON, B.G.J. (2003) Evolutionary stages of crystallization of weakly peralkaline syenites: evidence from ejecta in the plinian deposits of Agua de Pau volcano (São Miguel, Azores Islands). *Mineralogical Magazine* **67**, 749-767.

ROBINSON, K., GIBBS, G.V., & RIBBE, P.H. (1971) Quadratic elongation: a quantitative measure of distortion in coordination polyhedra. *Science* **171**, 567-570.

ROBLES, E.R., FONTAIN, F., MONCHOUX, P., SØRENSEN, H., & DE PARSEVAL, P. (2001) Hiortdahlite II from the Ilímaussaq alkaline complex, South Greenland, the Tamazeght complex, Morocco, and the Iles de Los, Guinea. *Geology of Greenland Survey Bulletin* **190**, 131-137.

SABURI, S., KAWAHARA, A., HENMI, C., KUSACHI, I., & KIHARA, K. (1977) The refinement of the crystal structure of cuspidine. *Mineralogical Journal* **8**, 286-298.

SCHEERER, T. (1843) Ueber den Wöhlerit, eine neue Mineralspecies. *Annalen der Physik und Chemie* **59**, 327-336.

SHANNON, R.D. & PREWITT, C.T. (1969) Effective ionic radii in oxides and fluorides. *Acta Crystallographica* **B25**, 925-946.

SHELDRICK, G.M. (2008) A short history of SHELX. *Acta Crystallographica* **A64**, 112-122.

SOKOLOVA, E. (2006) From structure topology to chemical composition. I. Structural hierarchy and stereochemistry in titanium disilicate minerals. *Canadian Mineralogist* **44**, 1273- 1330.

SOKOLOVA, E. & HAWTHORNE, F.C. (2008) From structure topology to chemical composition. V. Titanium silicates: the crystal chemistry of nacareniobsite-(Ce). *Canadian Mineralogist* **46**, 1333-1342.

SUBBOTIN, V.V., MERLINO, S., PUSHCHAROVSKY, D.Y., PAKHOMOVSKY, Y.A., FERRO, O., BOGDANOVA, A.N., VOLOSHIN, A.V., SOROKHTINA, N.V., & ZUBKOVA, N.V. (2000) Tumchaite $Na_2(Zr,Sn)Si_4O_{11}\times 2H_2O$ – A new mineral from carbonatites of the Vuoriyarvi alkali-ultrabasic massif, Murmansk Region, Russia. *American Mineralogist* **85**, 1516-1520.

SVESHNIKOVA, E.V. & BUROVA, T.A. (1973) Minerals of the wöhlerite group and titan-rosenbuschite from nepheline syenite of Trans-Angara. *Trudy Mineralogicheskiy Muzeya Akademiya Nauk SSSR* **22**, 119-123 (in Russian).

VLASOV, K.A., KUZ'MENKO, M.V., & ESKOVA, E.M. (1966) *The Lovozero alkaline massif*. Oliver and Boyde, Endinburgh and London.

WOOLLEY, A.R. & PLATT, R.G. (1986) The mineralogy of nepheline syenite complexes from the northern part of the Chilwa Province, Malawi. *Mineralogical Magazine*, **50**, 597-610.

Received December 22, 2011, revised manuscript accepted June 13, 2012.

```
data_wohlelos

_audit_creation_method           SHELXL-97
_chemical_name_systematic
;
 ?
;
_chemical_name_common            ?
_chemical_melting_point          ?
_chemical_formula_moiety         ?
_chemical_formula_sum
 'Ca7.68 F5 Fe0.80 Mn0.23 Na3.47 Nb0.92 O31 Si8 Ti1.08 Zr1.77'
_chemical_formula_weight         1559.49

loop_
 _atom_type_symbol
 _atom_type_description
 _atom_type_scat_dispersion_real
 _atom_type_scat_dispersion_imag
 _atom_type_scat_source
 'O'  'O'   0.0106   0.0060
 'International Tables Vol C Tables 4.2.6.8 and 6.1.1.4'
 'F'  'F'   0.0171   0.0103
 'International Tables Vol C Tables 4.2.6.8 and 6.1.1.4'
 'Si'  'Si'   0.0817   0.0704
 'International Tables Vol C Tables 4.2.6.8 and 6.1.1.4'
 'Ca'  'Ca'   0.2262   0.3064
 'International Tables Vol C Tables 4.2.6.8 and 6.1.1.4'
 'Na'  'Na'   0.0362   0.0249
 'International Tables Vol C Tables 4.2.6.8 and 6.1.1.4'
 'Zr'  'Zr'  -2.9673   0.5597
 'International Tables Vol C Tables 4.2.6.8 and 6.1.1.4'
 'Nb'  'Nb'  -2.0727   0.6215
 'International Tables Vol C Tables 4.2.6.8 and 6.1.1.4'
 'Fe'  'Fe'   0.3463   0.8444
 'International Tables Vol C Tables 4.2.6.8 and 6.1.1.4'
 'Mn'  'Mn'   0.3368   0.7283
 'International Tables Vol C Tables 4.2.6.8 and 6.1.1.4'
 'Ti'  'Ti'   0.2776   0.4457
 'International Tables Vol C Tables 4.2.6.8 and 6.1.1.4'
 'Mg'  'Mg'   0.0486   0.0363
 'International Tables Vol C Tables 4.2.6.8 and 6.1.1.4'

_symmetry_cell_setting           ?
_symmetry_space_group_name_H-M    'P 21'

loop_
 _symmetry_equiv_pos_as_xyz
 'x, y, z'
 '-x, y+1/2, -z'

_cell_length_a                   10.80498(16)
```

```
_cell_length_b                  10.25458(13)
_cell_length_c                  7.28606(10)
_cell_angle_alpha               90.00
_cell_angle_beta                109.1168(6)
_cell_angle_gamma               90.00
_cell_volume                    762.779(18)
_cell_formula_units_Z           1
_cell_measurement_temperature   293(2)
_cell_measurement_reflns_used   ?
_cell_measurement_theta_min     ?
_cell_measurement_theta_max     ?

_exptl_crystal_description      ?
_exptl_crystal_colour           'yellow'
_exptl_crystal_size_max         0.17
_exptl_crystal_size_mid         0.10
_exptl_crystal_size_min         0.04
_exptl_crystal_density_meas     ?
_exptl_crystal_density_diffrn   3.395
_exptl_crystal_density_method   'not measured'
_exptl_crystal_F_000            756.4
_exptl_absorpt_coefficient_mu   3.468
_exptl_absorpt_correction_type  'multi-scan'
_exptl_absorpt_correction_T_min 0.742
_exptl_absorpt_correction_T_max 0.902
_exptl_absorpt_process_details  ?

_exptl_special_details
;
 ?
;

_diffrn_ambient_temperature     293(2)
_diffrn_radiation_wavelength    0.71073
_diffrn_radiation_type          MoK\a
_diffrn_radiation_source        'fine-focus sealed tube'
_diffrn_radiation_monochromator graphite
_diffrn_measurement_device_type ?
_diffrn_measurement_method      ?
_diffrn_detector_area_resol_mean ?
_diffrn_standards_number        ?
_diffrn_standards_interval_count ?
_diffrn_standards_interval_time ?
_diffrn_standards_decay_%       ?
_diffrn_reflns_number           10017
_diffrn_reflns_av_R_equivalents 0.0141
_diffrn_reflns_av_sigmaI/netI   0.0246
_diffrn_reflns_limit_h_min      -16
_diffrn_reflns_limit_h_max      16
_diffrn_reflns_limit_k_min      -15
_diffrn_reflns_limit_k_max      15
_diffrn_reflns_limit_l_min      -11
_diffrn_reflns_limit_l_max      9
_diffrn_reflns_theta_min        2.82
```

```
_diffrn_reflns_theta_max         32.58
_reflns_number_total             5269
_reflns_number_gt                5013
_reflns_threshold_expression     >2sigma(I)

_computing_data_collection       ?
_computing_cell_refinement       ?
_computing_data_reduction        ?
_computing_structure_solution    ?
_computing_structure_refinement  'SHELXL-97 (Sheldrick, 1997)'
_computing_molecular_graphics    ?
_computing_publication_material  ?

_refine_special_details
;
 Refinement of F^2^ against ALL reflections.  The weighted R-factor wR and
 goodness of fit S are based on F^2^, conventional R-factors R are based
 on F, with F set to zero for negative F^2^. The threshold expression of
 F^2^ > 2sigma(F^2^) is used only for calculating R-factors(gt) etc. and is
 not relevant to the choice of reflections for refinement.  R-factors based
 on F^2^ are statistically about twice as large as those based on F, and R-
 factors based on ALL data will be even larger.
;

_refine_ls_structure_factor_coef  Fsqd
_refine_ls_matrix_type           full
_refine_ls_weighting_scheme      calc
_refine_ls_weighting_details
 'calc w=1/[\s^2^(Fo^2^)+(0.0219P)^2^+0.2176P] where P=(Fo^2^+2Fc^2^)/3'
_atom_sites_solution_primary     direct
_atom_sites_solution_secondary   difmap
_atom_sites_solution_hydrogens   ''
_refine_ls_hydrogen_treatment    ''
_refine_ls_extinction_method     none
_refine_ls_extinction_coef       ?
_refine_ls_abs_structure_details
 'Flack H D (1983), Acta Cryst. A39, 876-881'
_refine_ls_abs_structure_Flack   0.998(15)
_refine_ls_number_reflns         5269
_refine_ls_number_parameters     280
_refine_ls_number_restraints     1
_refine_ls_R_factor_all          0.0212
_refine_ls_R_factor_gt           0.0192
_refine_ls_wR_factor_ref         0.0458
_refine_ls_wR_factor_gt          0.0450
_refine_ls_goodness_of_fit_ref   1.028
_refine_ls_restrained_S_all      1.028
_refine_ls_shift/su_max          0.001
_refine_ls_shift/su_mean         0.000

loop_
 _atom_site_label
 _atom_site_type_symbol
 _atom_site_fract_x
```

```
 _atom_site_fract_y
 _atom_site_fract_z
 _atom_site_U_iso_or_equiv
 _atom_site_adp_type
 _atom_site_occupancy
 _atom_site_symmetry_multiplicity
 _atom_site_calc_flag
 _atom_site_refinement_flags
 _atom_site_disorder_assembly
 _atom_site_disorder_group
Ca1 Ca 0.34587(4) 0.29856(6) 0.55109(6) 0.01293(13) Uani 0.991(2) 1 d P . .
Nb Nb 0.12664(3) 0.05439(3) 0.18665(4) 0.01356(9) Uani 0.461(3) 1 d P . .
Ti Ti 0.12664(3) 0.05439(3) 0.18665(4) 0.01356(9) Uani 0.539(3) 1 d P . .
Zr Zr 0.34331(2) 0.28845(2) 0.05357(3) 0.00842(6) Uani 0.884(5) 1 d P . .
Mn Mn 0.34331(2) 0.28845(2) 0.05357(3) 0.00842(6) Uani 0.116(5) 1 d P . .
Ca2 Ca 0.14530(4) 0.68454(4) 0.19921(5) 0.01093(10) Uani 0.629(6) 1 d P . .
Fe2 Fe 0.14530(4) 0.68454(4) 0.19921(5) 0.01093(10) Uani 0.371(6) 1 d P . .
Ca3 Ca 0.36868(4) 0.91202(5) 0.05497(6) 0.01136(13) Uani 0.985(3) 1 d P . .
Ca4 Ca 0.15256(4) 0.68285(4) 0.69964(6) 0.01144(11) Uani 0.969(6) 1 d P . .
Fe4 Fe 0.15256(4) 0.68285(4) 0.69964(6) 0.01144(11) Uani 0.031(6) 1 d P . .
Na1 Na 0.12071(9) 0.06860(9) 0.68802(13) 0.0185(3) Uani 0.822(7) 1 d P . .
Ca1B Ca 0.12071(9) 0.06860(9) 0.68802(13) 0.0185(3) Uani 0.178(7) 1 d P . .
Na2 Na 0.36610(9) 0.91639(10) 0.55095(13) 0.0161(4) Uani 0.911(7) 1 d P . .
Ca2B Ca 0.36610(9) 0.91639(10) 0.55095(13) 0.0161(4) Uani 0.089(7) 1 d P . .
Si1 Si 0.08083(5) 0.37295(6) 0.19737(8) 0.00813(11) Uani 1 1 d . . .
Si2 Si 0.07316(5) 0.36510(6) 0.63719(8) 0.00815(11) Uani 1 1 d . . .
Si3 Si 0.43726(6) 0.61300(6) 0.56187(8) 0.00839(11) Uani 1 1 d . . .
Si4 Si 0.43164(5) 0.61251(6) 0.12396(8) 0.00783(11) Uani 1 1 d . . .
O1 O 0.00622(16) 0.23828(15) 0.1161(2) 0.0141(3) Uani 1 1 d . . .
O2 O -0.01991(15) 0.24162(15) 0.6198(2) 0.0131(3) Uani 1 1 d . . .
O3 O 0.00954(17) 0.50333(16) 0.0921(2) 0.0177(3) Uani 1 1 d . . .
O4 O 0.01860(16) 0.50030(16) 0.6918(3) 0.0186(3) Uani 1 1 d . . .
O5 O 0.23359(15) 0.37046(16) 0.2074(2) 0.0157(3) Uani 1 1 d . . .
O6 O 0.22203(15) 0.33521(18) 0.7763(2) 0.0170(3) Uani 1 1 d . . .
O7 O 0.48720(16) 0.47122(15) 0.6491(2) 0.0146(3) Uani 1 1 d . . .
O8 O 0.45854(16) 0.46462(15) 0.0736(2) 0.0146(3) Uani 1 1 d . . .
O9 O 0.47547(15) 0.23540(15) 0.3190(2) 0.0134(3) Uani 1 1 d . . .
O10 O 0.46701(16) 0.21858(16) 0.9125(2) 0.0165(3) Uani 1 1 d . . .
O11 O 0.28510(16) 0.64045(19) 0.5127(3) 0.0199(4) Uani 1 1 d . . .
O12 O 0.28695(16) 0.66807(17) 0.0247(2) 0.0163(3) Uani 1 1 d . . .
O13 O 0.24870(16) 0.11496(16) 0.0376(2) 0.0236(3) Uani 0.50 1 d P . .
F13 F 0.24870(16) 0.11496(16) 0.0376(2) 0.0236(3) Uani 0.50 1 d P . .
O14 O 0.22732(15) 0.11474(15) 0.4465(2) 0.0214(3) Uani 0.50 1 d P . .
F14 F 0.22732(15) 0.11474(15) 0.4465(2) 0.0214(3) Uani 0.50 1 d P . .
F15 F 0.23863(13) 0.88857(13) 0.74341(19) 0.0141(3) Uani 1 1 d . . .
O16 O 0.21728(16) 0.89070(14) 0.2255(2) 0.0177(3) Uani 0.50 1 d P . .
F16 F 0.21728(16) 0.89070(14) 0.2255(2) 0.0177(3) Uani 0.50 1 d P . .
O17 O 0.08994(19) 0.38911(18) 0.4246(2) 0.0256(4) Uani 1 1 d . . .
O18 O 0.52382(16) 0.12368(17) 0.6391(2) 0.0175(3) Uani 1 1 d . . .

loop_
 _atom_site_aniso_label
 _atom_site_aniso_U_11
 _atom_site_aniso_U_22
```

_atom_site_aniso_U_33
_atom_site_aniso_U_23
_atom_site_aniso_U_13
_atom_site_aniso_U_12
Ca1 0.0127(2) 0.0129(3) 0.0130(2) -0.00152(16) 0.00387(14) -0.00341(17)
Nb 0.01936(15) 0.01017(14) 0.01389(14) -0.00142(9) 0.00918(10) -0.00359(11)
Ti 0.01936(15) 0.01017(14) 0.01389(14) -0.00142(9) 0.00918(10) -0.00359(11)
Zr 0.00740(10) 0.01101(10) 0.00665(9) 0.00046(7) 0.00204(6) 0.00177(8)
Mn 0.00740(10) 0.01101(10) 0.00665(9) 0.00046(7) 0.00204(6) 0.00177(8)
Ca2 0.01065(18) 0.01309(19) 0.00965(17) -0.00085(13) 0.00411(13) -0.00213(14)
Fe2 0.01065(18) 0.01309(19) 0.00965(17) -0.00085(13) 0.00411(13) -0.00213(14)
Ca3 0.0106(2) 0.0134(2) 0.0095(2) -0.00066(14) 0.00263(15) -0.00036(15)
Ca4 0.0114(2) 0.0118(2) 0.01091(19) -0.00037(14) 0.00326(15) -0.00142(16)
Fe4 0.0114(2) 0.0118(2) 0.01091(19) -0.00037(14) 0.00326(15) -0.00142(16)
Na1 0.0177(5) 0.0146(5) 0.0239(5) 0.0048(3) 0.0080(3) 0.0056(3)
Ca1B 0.0177(5) 0.0146(5) 0.0239(5) 0.0048(3) 0.0080(3) 0.0056(3)
Na2 0.0153(5) 0.0186(6) 0.0158(5) 0.0010(3) 0.0068(3) 0.0023(3)
Ca2B 0.0153(5) 0.0186(6) 0.0158(5) 0.0010(3) 0.0068(3) 0.0023(3)
Si1 0.0086(2) 0.0075(2) 0.0081(2) 0.0008(2) 0.00249(18) 0.00118(19)
Si2 0.0082(2) 0.0081(2) 0.0079(2) -0.0001(2) 0.00217(18) 0.00031(19)
Si3 0.0085(2) 0.0090(3) 0.0074(2) -0.00014(19) 0.00224(18) 0.0002(2)
Si4 0.0086(2) 0.0076(2) 0.0073(2) 0.00025(19) 0.00262(18) 0.00013(19)
O1 0.0144(7) 0.0111(7) 0.0152(7) -0.0018(5) 0.0028(6) -0.0041(6)
O2 0.0127(7) 0.0116(6) 0.0151(7) -0.0009(5) 0.0044(5) -0.0022(6)
O3 0.0188(8) 0.0114(7) 0.0204(8) 0.0041(6) 0.0030(6) 0.0064(6)
O4 0.0153(7) 0.0104(7) 0.0322(9) -0.0051(6) 0.0107(7) -0.0009(6)
O5 0.0104(6) 0.0180(7) 0.0202(8) -0.0013(6) 0.0072(5) 0.0004(6)
O6 0.0097(7) 0.0232(8) 0.0149(7) 0.0045(6) -0.0001(6) 0.0020(6)
O7 0.0158(7) 0.0086(7) 0.0143(7) 0.0028(5) -0.0021(6) -0.0017(5)
O8 0.0160(7) 0.0093(7) 0.0222(8) -0.0024(6) 0.0113(6) -0.0014(6)
O9 0.0146(7) 0.0110(7) 0.0121(7) 0.0035(5) 0.0009(5) 0.0006(5)
O10 0.0186(8) 0.0158(7) 0.0179(7) -0.0024(6) 0.0097(6) 0.0049(6)
O11 0.0093(7) 0.0300(10) 0.0202(8) -0.0017(7) 0.0045(6) 0.0035(6)
O12 0.0107(7) 0.0172(7) 0.0179(8) 0.0011(6) 0.0005(5) 0.0023(6)
O13 0.0244(8) 0.0148(7) 0.0259(8) 0.0017(6) 0.0007(6) -0.0031(6)
F13 0.0244(8) 0.0148(7) 0.0259(8) 0.0017(6) 0.0007(6) -0.0031(6)
O14 0.0198(7) 0.0147(7) 0.0320(9) -0.0062(6) 0.0119(6) -0.0056(6)
F14 0.0198(7) 0.0147(7) 0.0320(9) -0.0062(6) 0.0119(6) -0.0056(6)
F15 0.0149(6) 0.0121(6) 0.0136(6) 0.0011(4) 0.0021(4) 0.0003(5)
O16 0.0257(8) 0.0116(6) 0.0184(7) -0.0012(5) 0.0106(6) -0.0047(6)
F16 0.0257(8) 0.0116(6) 0.0184(7) -0.0012(5) 0.0106(6) -0.0047(6)
O17 0.0395(11) 0.0294(10) 0.0099(7) -0.0015(7) 0.0110(7) -0.0090(8)
O18 0.0196(8) 0.0247(8) 0.0086(6) 0.0015(6) 0.0051(5) 0.0036(7)

```
data_normandite

_audit_creation_method           SHELXL-97
_chemical_name_systematic
;
 ?
;
_chemical_name_common             ?
_chemical_melting_point          ?
_chemical_formula_moiety          ?
_chemical_formula_sum
 'Ca3.30 F4 Mn2.90 Na4.70 O32 Si8 Ti4.30 Zr0.80'
_chemical_formula_weight          1491.11

loop_
 _atom_type_symbol
 _atom_type_description
 _atom_type_scat_dispersion_real
 _atom_type_scat_dispersion_imag
 _atom_type_scat_source
 'O'  'O'   0.0106   0.0060
 'International Tables Vol C Tables 4.2.6.8 and 6.1.1.4'
 'F'  'F'   0.0171   0.0103
 'International Tables Vol C Tables 4.2.6.8 and 6.1.1.4'
 'Si'  'Si'   0.0817   0.0704
 'International Tables Vol C Tables 4.2.6.8 and 6.1.1.4'
 'Ca'  'Ca'   0.2262   0.3064
 'International Tables Vol C Tables 4.2.6.8 and 6.1.1.4'
 'Mn'  'Mn'   0.3368   0.7283
 'International Tables Vol C Tables 4.2.6.8 and 6.1.1.4'
 'Zr'  'Zr'  -2.9673   0.5597
 'International Tables Vol C Tables 4.2.6.8 and 6.1.1.4'
 'Na'  'Na'   0.0362   0.0249
 'International Tables Vol C Tables 4.2.6.8 and 6.1.1.4'
 'Ti'  'Ti'   0.2776   0.4457
 'International Tables Vol C Tables 4.2.6.8 and 6.1.1.4'
 'Fe'  'Fe'   0.3463   0.8444
 'International Tables Vol C Tables 4.2.6.8 and 6.1.1.4'
 'Nb'  'Nb'  -2.0727   0.6215
 'International Tables Vol C Tables 4.2.6.8 and 6.1.1.4'

_symmetry_cell_setting            ?
_symmetry_space_group_name_H-M    P21/a

loop_
 _symmetry_equiv_pos_as_xyz
 'x, y, z'
 'x+1/2, -y+1/2, z'
 '-x, -y, -z'
 '-x-1/2, y-1/2, -z'

_cell_length_a                    10.8044(7)
```

```
_cell_length_b                  9.7945(7)
_cell_length_c                  7.0532(5)
_cell_angle_alpha               90.00
_cell_angle_beta                108.056(3)
_cell_angle_gamma               90.00
_cell_volume                    709.64(8)
_cell_formula_units_Z           1
_cell_measurement_temperature   293(2)
_cell_measurement_reflns_used   ?
_cell_measurement_theta_min     ?
_cell_measurement_theta_max     ?

_exptl_crystal_description      ?
_exptl_crystal_colour           ?
_exptl_crystal_size_max         0.45
_exptl_crystal_size_mid         0.06
_exptl_crystal_size_min         0.04
_exptl_crystal_density_meas     ?
_exptl_crystal_density_diffrn   3.489
_exptl_crystal_density_method   'not measured'
_exptl_crystal_F_000            720.8
_exptl_absorpt_coefficient_mu   3.841
_exptl_absorpt_correction_type  'multi-scan'
_exptl_absorpt_correction_T_min 0.758
_exptl_absorpt_correction_T_max 0.858
_exptl_absorpt_process_details  ?

_exptl_special_details
;
 ?
;

_diffrn_ambient_temperature     293(2)
_diffrn_radiation_wavelength    0.71073
_diffrn_radiation_type          MoK\a
_diffrn_radiation_source        'fine-focus sealed tube'
_diffrn_radiation_monochromator graphite
_diffrn_measurement_device_type ?
_diffrn_measurement_method      ?
_diffrn_detector_area_resol_mean ?
_diffrn_standards_number        ?
_diffrn_standards_interval_count ?
_diffrn_standards_interval_time ?
_diffrn_standards_decay_%       ?
_diffrn_reflns_number           9533
_diffrn_reflns_av_R_equivalents 0.0213
_diffrn_reflns_av_sigmaI/netI   0.0195
_diffrn_reflns_limit_h_min      -16
_diffrn_reflns_limit_h_max      15
_diffrn_reflns_limit_k_min      -14
_diffrn_reflns_limit_k_max      14
_diffrn_reflns_limit_l_min      -10
_diffrn_reflns_limit_l_max      10
_diffrn_reflns_theta_min        1.98
```

```
_diffrn_reflns_theta_max         32.61
_reflns_number_total             2625
_reflns_number_gt                2369
_reflns_threshold_expression     >2sigma(I)

_computing_data_collection       ?
_computing_cell_refinement       ?
_computing_data_reduction        ?
_computing_structure_solution    ?
_computing_structure_refinement  'SHELXL-97 (Sheldrick, 1997)'
_computing_molecular_graphics    ?
_computing_publication_material  ?

_refine_special_details
;
 Refinement of F^2^ against ALL reflections.  The weighted R-factor wR and
 goodness of fit S are based on F^2^, conventional R-factors R are based
 on F, with F set to zero for negative F^2^. The threshold expression of
 F^2^ > 2sigma(F^2^) is used only for calculating R-factors(gt) etc. and is
 not relevant to the choice of reflections for refinement.  R-factors based
 on F^2^ are statistically about twice as large as those based on F, and R-
 factors based on ALL data will be even larger.
;

_refine_ls_structure_factor_coef  Fsqd
_refine_ls_matrix_type           full
_refine_ls_weighting_scheme      calc
_refine_ls_weighting_details
 'calc w=1/[\s^2^(Fo^2^)+(0.0237P)^2^+0.5138P] where P=(Fo^2^+2Fc^2^)/3'
_atom_sites_solution_primary     direct
_atom_sites_solution_secondary   difmap
_atom_sites_solution_hydrogens   ''
_refine_ls_hydrogen_treatment    ''
_refine_ls_extinction_method     none
_refine_ls_extinction_coef       ?
_refine_ls_number_reflns         2625
_refine_ls_number_parameters     153
_refine_ls_number_restraints     0
_refine_ls_R_factor_all          0.0265
_refine_ls_R_factor_gt           0.0217
_refine_ls_wR_factor_ref         0.0536
_refine_ls_wR_factor_gt          0.0518
_refine_ls_goodness_of_fit_ref   1.089
_refine_ls_restrained_S_all      1.089
_refine_ls_shift/su_max          0.001
_refine_ls_shift/su_mean         0.000

loop_
 _atom_site_label
 _atom_site_type_symbol
 _atom_site_fract_x
 _atom_site_fract_y
 _atom_site_fract_z
 _atom_site_U_iso_or_equiv
```

```
 _atom_site_adp_type
 _atom_site_occupancy
 _atom_site_symmetry_multiplicity
 _atom_site_calc_flag
 _atom_site_refinement_flags
 _atom_site_disorder_assembly
 _atom_site_disorder_group
Zr1 Zr 0.28372(2) 0.10239(2) 0.02103(3) 0.00707(7) Uani 0.200(2) 1 d P . .
Ti1 Ti 0.28372(2) 0.10239(2) 0.02103(3) 0.00707(7) Uani 0.800(2) 1 d P . .
Mn2 Mn 0.43672(2) 0.36674(2) 0.85795(3) 0.01098(7) Uani 0.725(9) 1 d P . .
Ti2 Ti 0.43672(2) 0.36674(2) 0.85795(3) 0.01098(7) Uani 0.275(9) 1 d P . .
Ca3 Ca 0.30036(3) 0.10841(4) 0.52440(5) 0.01164(13) Uani 0.706(5) 1 d P . .
Na3 Na 0.30036(3) 0.10841(4) 0.52440(5) 0.01164(13) Uani 0.294(5) 1 d P . .
Ca4 Ca 0.42433(6) 0.37808(6) 0.33840(8) 0.0163(3) Uani 0.118(5) 1 d P . .
Na4 Na 0.42433(6) 0.37808(6) 0.33840(8) 0.0163(3) Uani 0.882(5) 1 d P . .
Si1 Si 0.62040(4) 0.16354(4) 0.21053(5) 0.00707(8) Uani 1 1 d . . .
Si2 Si 0.62101(4) 0.16562(4) 0.67011(5) 0.00709(8) Uani 1 1 d . . .
O1 O 0.64377(11) 0.15860(12) 0.45145(15) 0.0155(2) Uani 1 1 d . . .
O2 O 0.73935(10) 0.26300(10) 0.20008(15) 0.01168(19) Uani 1 1 d . . .
O3 O 0.74623(10) 0.25438(11) 0.80128(15) 0.01174(19) Uani 1 1 d . . .
O4 O 0.65222(11) 0.00956(10) 0.15779(16) 0.0127(2) Uani 1 1 d . . .
O5 O 0.63326(11) 0.00772(10) 0.74318(15) 0.0127(2) Uani 1 1 d . . .
O6 O 0.47691(10) 0.21983(10) 0.09716(15) 0.01102(19) Uani 1 1 d . . .
O7 O 0.48457(10) 0.23613(11) 0.64759(16) 0.0125(2) Uani 1 1 d . . .
O8 O 0.62659(10) 0.47435(11) 0.95688(16) 0.0130(2) Uani 1 1 d . . .
F9 F 0.38993(9) 0.50585(10) 0.60015(14) 0.01656(19) Uani 1 1 d . . .

loop_
 _atom_site_aniso_label
 _atom_site_aniso_U_11
 _atom_site_aniso_U_22
 _atom_site_aniso_U_33
 _atom_site_aniso_U_23
 _atom_site_aniso_U_13
 _atom_site_aniso_U_12
Zr1 0.00842(11) 0.00559(10) 0.00718(10) 0.00035(6) 0.00239(7) 0.00106(7)
Ti1 0.00842(11) 0.00559(10) 0.00718(10) 0.00035(6) 0.00239(7) 0.00106(7)
Mn2 0.01173(12) 0.01034(11) 0.01100(11) -0.00023(7) 0.00372(8) -0.00066(8)
Ti2 0.01173(12) 0.01034(11) 0.01100(11) -0.00023(7) 0.00372(8) -0.00066(8)
Ca3 0.01096(19) 0.01173(19) 0.01180(18) -0.00074(10) 0.00291(12) -0.00238(12)
Na3 0.01096(19) 0.01173(19) 0.01180(18) -0.00074(10) 0.00291(12) -0.00238(12)
Ca4 0.0162(4) 0.0163(3) 0.0164(3) -0.0018(2) 0.0050(2) -0.0041(2)
Na4 0.0162(4) 0.0163(3) 0.0164(3) -0.0018(2) 0.0050(2) -0.0041(2)
Si1 0.00745(17) 0.00691(17) 0.00680(16) 0.00022(11) 0.00212(12) 0.00045(12)
Si2 0.00710(17) 0.00673(16) 0.00720(16) 0.00006(11) 0.00184(12) -0.00017(12)
O1 0.0173(5) 0.0223(6) 0.0075(4) 0.0006(4) 0.0045(4) 0.0010(4)
O2 0.0106(5) 0.0099(4) 0.0148(5) 0.0027(3) 0.0043(4) -0.0007(4)
O3 0.0098(5) 0.0114(4) 0.0129(4) -0.0037(3) 0.0018(4) -0.0017(4)
O4 0.0161(5) 0.0079(4) 0.0151(5) -0.0015(3) 0.0062(4) 0.0016(4)
O5 0.0151(5) 0.0091(4) 0.0129(5) 0.0028(3) 0.0028(4) 0.0009(4)
O6 0.0088(4) 0.0109(5) 0.0126(4) 0.0016(3) 0.0021(3) 0.0009(4)
O7 0.0087(5) 0.0107(5) 0.0175(5) -0.0017(3) 0.0033(4) 0.0004(4)
O8 0.0097(5) 0.0133(5) 0.0155(5) 0.0023(3) 0.0030(4) 0.0016(4)
F9 0.0120(4) 0.0151(4) 0.0211(4) -0.0008(3) 0.0030(3) 0.0015(3)
```

```
data_lavelos2

_audit_creation_method           SHELXL-97
_chemical_name_systematic
;
 ?
;
_chemical_name_common            ?
_chemical_melting_point          ?
_chemical_formula_moiety         ?
_chemical_formula_sum
 'Ca1.64 F2.5 Mn1.58 Na2.36 O15.5 Si4 Ti0.96 Zr1.46'
_chemical_formula_weight         793.78

loop_
 _atom_type_symbol
 _atom_type_description
 _atom_type_scat_dispersion_real
 _atom_type_scat_dispersion_imag
 _atom_type_scat_source
 'O'  'O'   0.0106   0.0060
 'International Tables Vol C Tables 4.2.6.8 and 6.1.1.4'
 'F'  'F'   0.0171   0.0103
 'International Tables Vol C Tables 4.2.6.8 and 6.1.1.4'
 'Si'  'Si'   0.0817   0.0704
 'International Tables Vol C Tables 4.2.6.8 and 6.1.1.4'
 'Ca'  'Ca'   0.2262   0.3064
 'International Tables Vol C Tables 4.2.6.8 and 6.1.1.4'
 'Mn'  'Mn'   0.3368   0.7283
 'International Tables Vol C Tables 4.2.6.8 and 6.1.1.4'
 'Zr'  'Zr'  -2.9673   0.5597
 'International Tables Vol C Tables 4.2.6.8 and 6.1.1.4'
 'Na'  'Na'   0.0362   0.0249
 'International Tables Vol C Tables 4.2.6.8 and 6.1.1.4'
 'Ti'  'Ti'   0.2776   0.4457
 'International Tables Vol C Tables 4.2.6.8 and 6.1.1.4'
 'Fe'  'Fe'   0.3463   0.8444
 'International Tables Vol C Tables 4.2.6.8 and 6.1.1.4'
 'Nb'  'Nb'  -2.0727   0.6215
 'International Tables Vol C Tables 4.2.6.8 and 6.1.1.4'

_symmetry_cell_setting           ?
_symmetry_space_group_name_H-M    P21/a

loop_
 _symmetry_equiv_pos_as_xyz
 'x, y, z'
 'x+1/2, -y+1/2, z'
 '-x, -y, -z'
 '-x-1/2, y-1/2, -z'

_cell_length_a                   10.8475(6)
```

```
_cell_length_b                  9.9364(6)
_cell_length_c                  7.1488(4)
_cell_angle_alpha               90.00
_cell_angle_beta                108.392(4)
_cell_angle_gamma               90.00
_cell_volume                    731.17(7)
_cell_formula_units_Z           2
_cell_measurement_temperature   293(2)
_cell_measurement_reflns_used   ?
_cell_measurement_theta_min     ?
_cell_measurement_theta_max     ?

_exptl_crystal_description      'prism'
_exptl_crystal_colour           'honey-yellow'
_exptl_crystal_size_max         0.20
_exptl_crystal_size_mid         0.08
_exptl_crystal_size_min         0.05
_exptl_crystal_density_meas     ?
_exptl_crystal_density_diffrn   3.607
_exptl_crystal_density_method   'not measured'
_exptl_crystal_F_000            760.5
_exptl_absorpt_coefficient_mu   3.947
_exptl_absorpt_correction_type  'multi-scan'
_exptl_absorpt_correction_T_min 0.691
_exptl_absorpt_correction_T_max 0.821
_exptl_absorpt_process_details  ?

_exptl_special_details
;
 ?
;

_diffrn_ambient_temperature     293(2)
_diffrn_radiation_wavelength    0.71073
_diffrn_radiation_type          MoK\a
_diffrn_radiation_source        'fine-focus sealed tube'
_diffrn_radiation_monochromator graphite
_diffrn_measurement_device_type ?
_diffrn_measurement_method      ?
_diffrn_detector_area_resol_mean ?
_diffrn_standards_number        ?
_diffrn_standards_interval_count ?
_diffrn_standards_interval_time ?
_diffrn_standards_decay_%       ?
_diffrn_reflns_number           9624
_diffrn_reflns_av_R_equivalents 0.0303
_diffrn_reflns_av_sigmaI/netI   0.0316
_diffrn_reflns_limit_h_min      -16
_diffrn_reflns_limit_h_max      16
_diffrn_reflns_limit_k_min      -14
_diffrn_reflns_limit_k_max      13
_diffrn_reflns_limit_l_min      -10
_diffrn_reflns_limit_l_max      10
_diffrn_reflns_theta_min        1.98
```

_diffrn_reflns_theta_max 32.50
_reflns_number_total 2665
_reflns_number_gt 2301
_reflns_threshold_expression >2sigma(I)

_computing_data_collection ?
_computing_cell_refinement ?
_computing_data_reduction ?
_computing_structure_solution ?
_computing_structure_refinement 'SHELXL-97 (Sheldrick, 1997)'
_computing_molecular_graphics ?
_computing_publication_material ?

_refine_special_details
;
Refinement of F^2^ against ALL reflections. The weighted R-factor wR and
goodness of fit S are based on F^2^, conventional R-factors R are based
on F, with F set to zero for negative F^2^. The threshold expression of
F^2^ > 2sigma(F^2^) is used only for calculating R-factors(gt) etc. and is
not relevant to the choice of reflections for refinement. R-factors based
on F^2^ are statistically about twice as large as those based on F, and R-
factors based on ALL data will be even larger.
;

_refine_ls_structure_factor_coef Fsqd
_refine_ls_matrix_type full
_refine_ls_weighting_scheme calc
_refine_ls_weighting_details
'calc w=1/[\s^2^(Fo^2^)+(0.0311P)^2^+18.6747P] where P=(Fo^2^+2Fc^2^)/3'
_atom_sites_solution_primary direct
_atom_sites_solution_secondary difmap
_atom_sites_solution_hydrogens ''
_refine_ls_hydrogen_treatment 'none'
_refine_ls_extinction_method SHELXL
_refine_ls_extinction_coef 0.0034(6)
_refine_ls_extinction_expression
'Fc^*^=kFc[1+0.001xFc^2^\l^3^/sin(2\q)]^-1/4^'
_refine_ls_number_reflns 2665
_refine_ls_number_parameters 154
_refine_ls_number_restraints 0
_refine_ls_R_factor_all 0.0711
_refine_ls_R_factor_gt 0.0571
_refine_ls_wR_factor_ref 0.1646
_refine_ls_wR_factor_gt 0.1499
_refine_ls_goodness_of_fit_ref 1.145
_refine_ls_restrained_S_all 1.145
_refine_ls_shift/su_max 0.000
_refine_ls_shift/su_mean 0.000

loop_
_atom_site_label
_atom_site_type_symbol
_atom_site_fract_x
_atom_site_fract_y

```
 _atom_site_fract_z
 _atom_site_U_iso_or_equiv
 _atom_site_adp_type
 _atom_site_occupancy
 _atom_site_symmetry_multiplicity
 _atom_site_calc_flag
 _atom_site_refinement_flags
 _atom_site_disorder_assembly
 _atom_site_disorder_group
Zr1 Zr 0.29416(7) 0.10458(7) 0.02461(11) 0.0126(2) Uani 0.733(13) 1 d P . .
Ti1 Ti 0.29416(7) 0.10458(7) 0.02461(11) 0.0126(2) Uani 0.267(13) 1 d P . .
Mn2 Mn 0.43681(10) 0.37260(11) 0.85520(18) 0.0153(3) Uani 0.79(4) 1 d P . .
Ti2 Ti 0.43681(10) 0.37260(11) 0.85520(18) 0.0153(3) Uani 0.21(4) 1 d P . .
Ca3 Ca 0.30325(16) 0.10791(19) 0.5262(3) 0.0179(7) Uani 0.60(2) 1 d P . .
Na3 Na 0.30325(16) 0.10791(19) 0.5262(3) 0.0179(7) Uani 0.40(2) 1 d P . .
Ca4 Ca 0.4263(2) 0.3797(3) 0.3416(4) 0.0213(10) Uani 0.22(2) 1 d P . .
Na4 Na 0.4263(2) 0.3797(3) 0.3416(4) 0.0213(10) Uani 0.78(2) 1 d P . .
Si1 Si 0.62284(16) 0.16655(18) 0.2174(3) 0.0106(4) Uani 1 1 d . . .
Si2 Si 0.61952(16) 0.16812(18) 0.6676(3) 0.0112(4) Uani 1 1 d . . .
O1 O 0.6374(6) 0.1668(8) 0.4516(9) 0.0315(14) Uani 1 1 d . . .
O2 O 0.7408(5) 0.2628(5) 0.2073(9) 0.0178(10) Uani 1 1 d . . .
O3 O 0.7470(5) 0.2508(6) 0.7990(9) 0.0207(11) Uani 1 1 d . . .
O4 O 0.6528(5) 0.0141(5) 0.1661(9) 0.0200(11) Uani 1 1 d . . .
O5 O 0.6288(5) 0.0122(5) 0.7351(9) 0.0213(11) Uani 1 1 d . . .
O6 O 0.4797(4) 0.2205(5) 0.0968(8) 0.0163(10) Uani 1 1 d . . .
O7 O 0.4854(5) 0.2396(6) 0.6534(10) 0.0242(12) Uani 1 1 d . . .
O8 O 0.6201(5) 0.4798(6) 0.9538(9) 0.0224(11) Uani 0.75 1 d P . .
F8 F 0.6201(5) 0.4798(6) 0.9538(9) 0.0224(11) Uani 0.25 1 d P . .
F9 F 0.3869(4) 0.5057(5) 0.5943(8) 0.0274(11) Uani 1 1 d . . .

loop_
 _atom_site_aniso_label
 _atom_site_aniso_U_11
 _atom_site_aniso_U_22
 _atom_site_aniso_U_33
 _atom_site_aniso_U_23
 _atom_site_aniso_U_13
 _atom_site_aniso_U_12
Zr1 0.0142(3) 0.0089(3) 0.0146(4) 0.0011(2) 0.0042(2) 0.0042(2)
Ti1 0.0142(3) 0.0089(3) 0.0146(4) 0.0011(2) 0.0042(2) 0.0042(2)
Mn2 0.0135(5) 0.0135(5) 0.0193(6) -0.0012(4) 0.0059(4) -0.0007(3)
Ti2 0.0135(5) 0.0135(5) 0.0193(6) -0.0012(4) 0.0059(4) -0.0007(3)
Ca3 0.0155(9) 0.0157(9) 0.0219(10) -0.0002(7) 0.0053(7) -0.0036(6)
Na3 0.0155(9) 0.0157(9) 0.0219(10) -0.0002(7) 0.0053(7) -0.0036(6)
Ca4 0.0181(13) 0.0220(15) 0.0240(15) -0.0026(10) 0.0069(10) -0.0064(9)
Na4 0.0181(13) 0.0220(15) 0.0240(15) -0.0026(10) 0.0069(10) -0.0064(9)
Si1 0.0078(7) 0.0100(7) 0.0137(8) 0.0003(6) 0.0028(6) 0.0001(6)
Si2 0.0092(7) 0.0092(7) 0.0145(8) 0.0001(6) 0.0029(6) 0.0004(5)
O1 0.033(3) 0.051(4) 0.011(2) 0.000(3) 0.008(2) -0.002(3)
O2 0.0104(19) 0.013(2) 0.029(3) 0.0037(19) 0.0051(18) -0.0023(16)
O3 0.014(2) 0.021(3) 0.025(3) -0.005(2) 0.0029(19) -0.0047(19)
O4 0.018(2) 0.013(2) 0.031(3) 0.000(2) 0.011(2) 0.0018(18)
O5 0.021(2) 0.013(2) 0.029(3) 0.005(2) 0.006(2) 0.0020(19)
O6 0.0071(18) 0.016(2) 0.023(2) 0.0023(19) 0.0005(17) 0.0014(16)
```

O7 0.013(2) 0.015(2) 0.044(4) -0.005(2) 0.007(2) 0.0009(18)
O8 0.014(2) 0.022(3) 0.030(3) 0.005(2) 0.0045(19) 0.0035(18)
F8 0.014(2) 0.022(3) 0.030(3) 0.005(2) 0.0045(19) 0.0035(18)
F9 0.0147(19) 0.023(2) 0.040(3) -0.004(2) 0.0019(19) 0.0025(17)

```
data_hiortlos

_audit_creation_method           SHELXL-97
_chemical_name_systematic
;
 ?
;
_chemical_name_common            ?
_chemical_melting_point          ?
_chemical_formula_moiety         ?
_chemical_formula_sum
 'Ca9.42 F6 Mn1.34 Na3.24 O30 Si8 Ti0.52 Zr1.48'
_chemical_formula_weight         1504.28

loop_
 _atom_type_symbol
 _atom_type_description
 _atom_type_scat_dispersion_real
 _atom_type_scat_dispersion_imag
 _atom_type_scat_source
 'Ca'  'Ca'   0.2262   0.3064
 'International Tables Vol C Tables 4.2.6.8 and 6.1.1.4'
 'Zr'  'Zr'  -2.9673   0.5597
 'International Tables Vol C Tables 4.2.6.8 and 6.1.1.4'
 'Ti'  'Ti'   0.2776   0.4457
 'International Tables Vol C Tables 4.2.6.8 and 6.1.1.4'
 'Mn'  'Mn'   0.3368   0.7283
 'International Tables Vol C Tables 4.2.6.8 and 6.1.1.4'
 'Fe'  'Fe'   0.3463   0.8444
 'International Tables Vol C Tables 4.2.6.8 and 6.1.1.4'
 'Na'  'Na'   0.0362   0.0249
 'International Tables Vol C Tables 4.2.6.8 and 6.1.1.4'
 'Si'  'Si'   0.0817   0.0704
 'International Tables Vol C Tables 4.2.6.8 and 6.1.1.4'
 'O'  'O'   0.0106   0.0060
 'International Tables Vol C Tables 4.2.6.8 and 6.1.1.4'
 'F'  'F'   0.0171   0.0103
 'International Tables Vol C Tables 4.2.6.8 and 6.1.1.4'

_symmetry_cell_setting           ?
_symmetry_space_group_name_H-M    P-1

loop_
 _symmetry_equiv_pos_as_xyz
 'x, y, z'
 '-x, -y, -z'

_cell_length_a                 10.934(3)
_cell_length_b                 10.991(7)
_cell_length_c                 7.366(2)
_cell_angle_alpha               109.43(2)
_cell_angle_beta                109.60(3)
```

```
_cell_angle_gamma                83.56(3)
_cell_volume                     786.4(6)
_cell_formula_units_Z            1
_cell_measurement_temperature    293(2)
_cell_measurement_reflns_used    ?
_cell_measurement_theta_min      ?
_cell_measurement_theta_max      ?

_exptl_crystal_description       ?
_exptl_crystal_colour            ?
_exptl_crystal_size_max          0.50
_exptl_crystal_size_mid          0.40
_exptl_crystal_size_min          0.36
_exptl_crystal_density_meas      ?
_exptl_crystal_density_diffrn    3.176
_exptl_crystal_density_method    'not measured'
_exptl_crystal_F_000             751
_exptl_absorpt_coefficient_mu    3.174
_exptl_absorpt_correction_type   'psi-scan'
_exptl_absorpt_correction_T_min  0.201
_exptl_absorpt_correction_T_max  0.281
_exptl_absorpt_process_details   'North et al.,1968'

_exptl_special_details
;
 ?
;

_diffrn_ambient_temperature      293(2)
_diffrn_radiation_wavelength     0.71073
_diffrn_radiation_type           MoK\a
_diffrn_radiation_source         'fine-focus sealed tube'
_diffrn_radiation_monochromator  graphite
_diffrn_measurement_device_type  ?
_diffrn_measurement_method       ?
_diffrn_detector_area_resol_mean ?
_diffrn_standards_number         ?
_diffrn_standards_interval_count ?
_diffrn_standards_interval_time  ?
_diffrn_standards_decay_%        ?
_diffrn_reflns_number            3129
_diffrn_reflns_av_R_equivalents  0.0444
_diffrn_reflns_av_sigmaI/netI    0.0442
_diffrn_reflns_limit_h_min       -1
_diffrn_reflns_limit_h_max       12
_diffrn_reflns_limit_k_min       -12
_diffrn_reflns_limit_k_max       12
_diffrn_reflns_limit_l_min       -8
_diffrn_reflns_limit_l_max       8
_diffrn_reflns_theta_min         1.96
_diffrn_reflns_theta_max         25.01
_reflns_number_total             2664
_reflns_number_gt                2360
_reflns_threshold_expression     >2sigma(I)
```

```
_computing_data_collection       ?
_computing_cell_refinement       ?
_computing_data_reduction        ?
_computing_structure_solution    ?
_computing_structure_refinement   'SHELXL-97 (Sheldrick, 1997)'
_computing_molecular_graphics    ?
_computing_publication_material   ?

_refine_special_details
;
 Refinement of F^2^ against ALL reflections.  The weighted R-factor wR and
 goodness of fit S are based on F^2^, conventional R-factors R are based
 on F, with F set to zero for negative F^2^. The threshold expression of
 F^2^ > 2sigma(F^2^) is used only for calculating R-factors(gt) etc. and is
 not relevant to the choice of reflections for refinement.  R-factors based
 on F^2^ are statistically about twice as large as those based on F, and R-
 factors based on ALL data will be even larger.
;

_refine_ls_structure_factor_coef  Fsqd
_refine_ls_matrix_type           full
_refine_ls_weighting_scheme      calc
_refine_ls_weighting_details
 'calc w=1/[\s^2^(Fo^2^)+(0.0326P)^2^+22.5852P] where P=(Fo^2^+2Fc^2^)/3'
_atom_sites_solution_primary     direct
_atom_sites_solution_secondary    difmap
_atom_sites_solution_hydrogens    ''
_refine_ls_hydrogen_treatment     ''
_refine_ls_extinction_method     none
_refine_ls_extinction_coef       ?
_refine_ls_number_reflns         2664
_refine_ls_number_parameters     186
_refine_ls_number_restraints     0
_refine_ls_R_factor_all          0.0840
_refine_ls_R_factor_gt           0.0727
_refine_ls_wR_factor_ref         0.1652
_refine_ls_wR_factor_gt          0.1581
_refine_ls_goodness_of_fit_ref   1.153
_refine_ls_restrained_S_all      1.153
_refine_ls_shift/su_max          0.059
_refine_ls_shift/su_mean         0.013

loop_
 _atom_site_label
 _atom_site_type_symbol
 _atom_site_fract_x
 _atom_site_fract_y
 _atom_site_fract_z
 _atom_site_U_iso_or_equiv
 _atom_site_adp_type
 _atom_site_occupancy
 _atom_site_symmetry_multiplicity
 _atom_site_calc_flag
```

_atom_site_refinement_flags
_atom_site_disorder_assembly
_atom_site_disorder_group
Ca1 Ca 0.4037(4) 0.3074(3) 0.2323(6) 0.0177(8) Uani 1 1 d . . .
Ca2 Ca 0.9026(3) 0.1936(4) 0.4233(5) 0.0134(9) Uani 1 1 d . . .
Ca3 Ca 0.8990(3) 0.1914(4) 0.9189(5) 0.0105(8) Uani 1 1 d . . .
Ca4 Ca 0.1284(4) 0.4233(4) 0.8945(6) 0.0128(14) Uani 0.84(4) 1 d P . .
Na4 Na 0.1284(4) 0.4233(4) 0.8945(6) 0.0128(14) Uani 0.16(4) 1 d P . .
Zr Zr 0.40303(18) 0.29429(18) 0.7216(3) 0.0104(6) Uani 0.74(2) 1 d P . .
Ti Ti 0.40303(18) 0.29429(18) 0.7216(3) 0.0104(6) Uani 0.26(2) 1 d P . .
M Mn 0.6272(3) 0.0665(3) 0.4786(4) 0.0181(10) Uani 0.67(5) 1 d P . .
M1 Ca 0.6272(3) 0.0665(3) 0.4786(4) 0.0181(10) Uani 0.33(5) 1 d P . .
Na Na 0.1230(6) 0.4226(6) 0.4007(10) 0.0099(14) Uani 1 1 d . . .
NaCA Na 0.6244(5) 0.0775(4) 0.9678(7) 0.0178(18) Uani 0.46(4) 1 d P . .
CaNA Ca 0.6244(5) 0.0775(4) 0.9678(7) 0.0178(18) Uani 0.54(4) 1 d P . .
Si1 Si 0.3339(4) 0.6215(5) 0.8215(8) 0.0143(12) Uani 1 1 d . . .
Si2 Si 0.3308(5) 0.6205(5) 0.3772(8) 0.0155(12) Uani 1 1 d . . .
Si3 Si 0.1837(5) 0.1270(5) 0.2475(7) 0.0167(12) Uani 1 1 d . . .
Si4 Si 0.1864(4) 0.1246(4) 0.8097(7) 0.0096(10) Uani 1 1 d . . .
O1 O 0.3582(12) 0.6203(11) 0.6123(19) 0.029(3) Uiso 1 1 d . . .
O2 O 0.2207(12) 0.1405(12) 0.0540(19) 0.033(3) Uiso 1 1 d . . .
O3 O 0.2713(12) 0.4886(12) 0.2303(19) 0.024(3) Uiso 1 1 d . . .
O4 O 0.0351(11) 0.1569(11) 0.7160(18) 0.022(3) Uiso 1 1 d . . .
O5 O 0.2297(11) 0.7396(11) 0.8684(18) 0.021(3) Uiso 1 1 d . . .
O6 O 0.0341(12) 0.1504(13) 0.219(2) 0.029(3) Uiso 1 1 d . . .
O7 O 0.4848(12) 0.1136(13) 0.6593(19) 0.023(3) Uiso 1 1 d . . .
O8 O 0.2446(12) 0.7481(11) 0.3599(19) 0.025(3) Uiso 1 1 d . . .
O9 O 0.2361(11) -0.0168(12) 0.7059(18) 0.024(3) Uiso 1 1 d . . .
O10 O 0.2747(11) 0.2430(11) 0.8412(18) 0.023(3) Uiso 1 1 d . . .
O11 O 0.5222(12) 0.3614(13) 0.6075(19) 0.027(3) Uiso 1 1 d . . .
O12 O 0.2857(12) 0.4761(12) 0.7751(19) 0.024(3) Uiso 1 1 d . . .
O13 O 0.2681(11) 0.2437(11) 0.4258(17) 0.021(3) Uiso 1 1 d . . .
O14 O 0.2408(11) -0.0148(11) 0.2585(17) 0.019(3) Uiso 1 1 d . . .
O15 O 0.5245(12) 0.3384(13) 0.0184(19) 0.027(3) Uiso 1 1 d . . .
F1 F -0.0077(10) 0.3908(10) 0.0598(15) 0.021(2) Uiso 1 1 d . . .
F2 F -0.0113(10) 0.3931(9) 0.5722(15) 0.021(2) Uiso 1 1 d . . .
F3 F 0.5035(10) 0.1136(11) 0.1930(17) 0.029(2) Uiso 1 1 d . . .

loop_
_atom_site_aniso_label
_atom_site_aniso_U_11
_atom_site_aniso_U_22
_atom_site_aniso_U_33
_atom_site_aniso_U_23
_atom_site_aniso_U_13
_atom_site_aniso_U_12
Ca1 0.0152(17) 0.016(2) 0.0182(18) 0.0014(17) 0.0065(14) 0.0039(17)
Ca2 0.0118(18) 0.0122(18) 0.0117(18) 0.0004(16) 0.0018(14) 0.0010(15)
Ca3 0.0097(17) 0.0105(17) 0.0105(17) -0.0001(15) 0.0044(13) -0.0032(14)
Ca4 0.012(2) 0.012(2) 0.013(2) 0.0018(17) 0.0060(15) 0.0036(16)
Na4 0.012(2) 0.012(2) 0.013(2) 0.0018(17) 0.0060(15) 0.0036(16)
Zr 0.0077(9) 0.0122(10) 0.0102(9) 0.0030(8) 0.0017(6) -0.0001(8)
Ti 0.0077(9) 0.0122(10) 0.0102(9) 0.0030(8) 0.0017(6) -0.0001(8)
M 0.0205(19) 0.0152(16) 0.0171(18) 0.0035(14) 0.0055(14) -0.0011(13)

M1 0.0205(19) 0.0152(16) 0.0171(18) 0.0035(14) 0.0055(14) -0.0011(13)
Na 0.009(3) 0.010(3) 0.009(3) -0.001(3) 0.006(3) 0.002(3)
NaCA 0.019(3) 0.015(3) 0.015(3) -0.002(2) 0.004(2) -0.009(2)
CaNA 0.019(3) 0.015(3) 0.015(3) -0.002(2) 0.004(2) -0.009(2)
Si1 0.009(2) 0.015(2) 0.018(3) 0.0052(18) 0.0040(18) -0.0004(17)
Si2 0.017(2) 0.009(2) 0.019(3) -0.0003(19) 0.008(2) 0.0007(17)
Si3 0.018(2) 0.016(2) 0.013(2) 0.0030(19) 0.001(2) -0.0014(19)
Si4 0.004(2) 0.006(2) 0.016(3) 0.0021(17) 0.0018(18) 0.0014(16)